UNIVERSITÀ DEGLI STUDI DI PADOVA

Dipartimento di Fisica e Astronomia "Galileo Galilei"
Master Degree in Astrophysics and Cosmology

Final dissertation

Analysis of the variability properties of the stars in the PLATO Input Catalogue

Thesis supervisor

Prof. Giampaolo Piotto

Thesis co-supervisor

Dr. Marco Montalto

Thesis external examiner

Dr. Silvano Desidera

Candidate

Adriana Barbieri

19/07/2023

Academic Year 2022/2023

Analysis of the variability properties of the stars in the PLATO Input Catalogue

Adriana Barbieri

Abstract

This thesis work examines the variability properties of a sample of stars included in the PLATO Input Catalogue, which has been selected through a cross-match operation with the variable sources in the Gaia Data Release 3. Particularly, the study focuses on the photometric, astrometric and spectroscopic data analysis of 11 specific classes of variable objects, and on the relevance of these sources for the PLATO space mission.
Finally, a comparison with several catalogues of variable objects from the literature is undertaken.

Dedication

Acknowledgements

This work has made use of data from the European Space Agency (ESA) mission *Gaia* processed by the *Gaia* Data Processing and Analysis Consortium (DPAC, `https://www.cosmos.esa.int/web/gaia/dpac/consortium`). Funding for the DPAC has been provided by national institutions, in particular the institutions participating in the *Gaia* Multilateral Agreement.
The Gaia mission website is `https://www.cosmos.esa.int/gaia`, the Gaia archive website is `https://archives.esac.esa.int/gaia`.
Some of the data presented in this work were obtained from the Mikulski Archive for Space Telescopes (MAST) at the Space Telescope Science Institute. STScI is operated by the Association of Universities for Research in Astronomy, Inc., under NASA contract NAS5–26555. Support to MAST for these data is provided by the NASA Office of Space Science via grant NAG5–7584 and by other grants and contracts.
The All-sky PLATO Input Catalogue (asPIC) can be accessed via `https://doi.org/10.17909/t9-8msm-xh08`.

Contents

List of Figures

List of Tables

Introduction

Chapter 1

PLATO space mission

1.1 Mission overview

1.1.1 Scientific objectives

1.1.2 Instrumentation and payload

1.1.3 Mission design

1.2 PLATO Input Catalogue

(Montalto et al. 2021)

1.3 Long-duration Observation Phase field selection

(Nascimbeni et al. 2022)

1.4 PLATO Roadmap and legacy

Chapter 2

Gaia space mission

2.1 Mission overview

(Gaia Collaboration, Prusti, et al. 2016)

2.1.1 Scientific objectives

2.1.2 Instrumentation and payload

2.1.3 Mission design

2.2 Gaia Data Release 3

(Gaia Collaboration, Vallenari, et al. 2022)

2.3 Variability and Specific Object Studies modules

As stated in Rimoldini et al. 2022, time-dependent brightness variations of celestial objects may be caused by different phenomena, and a certain set of classes can be identified to describe different variability types. Indeed Gaia offers the unique opportunity to study variability of close to 2 billion objects: its multi-epoch observations and sparse sampling allow for the detection of periodic signals ranging from minutes to years and for medium to long-term

non-periodic variability.

Among the strong points of the mission for variability analysis, we can mention, in addition to its well-known astrometric capabilities, the large dynamical range reached in stellar brightness, from a few magnitudes to fainter than 20 mag, the specific scanning law leading to irregularly sampled time series, and the quasi-simultaneity (within tens of seconds) of the observations in G photometry, G_{BP} and G_{RP} spectrophotometry, and RVS (Radial Velocity Spectrometer) spectroscopy.

2.4 Gaia Roadmap and legacy

Chapter 3

Variability analysis

3.1 Preliminary data analysis

Variability analysis can be defined as the comprehensive assessment of the degree and character of patterns of variation of the source's brightness over time intervals.

In this thesis work I analyzed two sample of stars obtained from the two outer regions centered on the Long-duration Observation Phase (LOP) north and south fields in the PLATO Input Catalogue, selected as explained in Nascimbeni et al. 2022.

These outer caps count respectively 543394 and 593563 targets, that have been cross-matched by the unique source identifier *source_id* with each variable source of the 11 Specific Object Studies (SOS) modules in Gaia Data Release 3.
As described in Eyer et al. 2022 and section 2, these variability classes include RR Lyrae stars, Cepheids, eclipsing binaries, upper Main Sequence oscillators, solar-like variables with rotational modulation, short timescale variables, long period variables, active galactic nuclei, microlensing events, compact companions and stellar hosts of transiting extra-solar planets.

Following the cross-matching operation, the resulting non-null variability classes have been complemented with selected photometric, spectroscopic, astrometric and astrophysical parameters of the sources, obtained via ADQL (Astronomical Data Query Language) Advanced Search in the Gaia Archive query interface.

Non tabular data such as epoch photometry in the G, G_{BP} , and G_{RP} bands and mean

Variability class	LOPN1	LOPS2
Short timescale	2996	4081
Eclipsing binaries	2977	3467
Solar-like	1794	1849
MS oscillators	153	438
RR Lyrae	84	78
Exoplanetary hosts	21	31
Cepheids	1	0
Long period	0	1

Table 3.1: Variable sources in the PIC outer LOP fields.

spectra have instead been extracted via DataLink from the Gaia Archive.

The outcome of this preliminary analysis is the distribution of several classes of variable objects in the all-sky PLATO Input Catalogue that is reported in table 3.1.

No Active Galactic Nuclei, microlensing events and compact companions are collected in the PLATO Input Catalogue.

The main parameters selected for each of the aforementioned classes of variable objects have been collected in Tables 3.2a and 3.2b.

The all-sky distribution of the different classes of variable sources in Aitoff projection and Galactic coordinates is displayed in Figure 3.1, while the absolute Color-Magnitude Diagrams corrected for extinction are shown in 3.2.

For each variability class, sky map distributions, observational Hertzsprung–Russell diagrams, and photometric time series have been obtained.

Moreover in order to characterize variability the statistics of photometric time series have been exploited, such as the Abbe value and the skewness magnitude for G FoV transits, that together constitude a metric targeting non-periodic variations. The Abbe value, or von-Neumann ratio statistic, measures the point-to-point scatter in a photometric time series, and is an estimate of the regularity of the light curve variability pattern over the duration of the observations; in other words it estimates the smoothness of the light curve. The skewness of the magnitude distribution is instead a measure of the asymmetry of the light curve. A metric targeting periodic variations is given by the distribution of the ratio of the two bands

mean photometric uncertainties as a function of the median magnitude in the G band, where stellar pulsations are expected to exhibit larger variations in the G_{BP} than in the G_{RP} band.

In the following sections the main properties of the variable sources located in the northern and southern outer LOP fields are investigated.

	Variability types			
gaiadr3. tables	**RR Lyrae**	**Cepheids**	**planetary transits**	**eclipsing binaries**
gaia_source	l	l	l	l
gaia_source	b	b	b	b
gaia_source	parallax	parallax	parallax	parallax
vari_summary	median_mag_g_fov	median_mag_g_fov	median_mag_g_fov	median_mag_g_fov
vari_summary	median_mag_bp	median_mag_bp	median_mag_bp	median_mag_bp
vari_summary	median_mag_rp	median_mag_rp	median_mag_rp	median_mag_rp
astrophysical_parameters	ag_gspphot		ag_gspphot	ag_gspphot
vari_type	source_id	source_id	source_id	source_id
vari_type	p_f	p_f	transit_period	frequency
vari_type	p1_o	p1_o		
vari_type	peak_to_peak_g			
vari_type	metallicity			
vari_type	best_classification	type_best_classification		
vari_type	reference_time_g	reference_time_g	transit_reference_time	reference_time
vari_type	reference_time_bp	reference_time_bp		
vari_type	reference_time_rp	reference_time_rp		
vari_type	reference_time_rv			
datalink	epoch photometry (G, BP, RP time series)	epoch photometry (G, BP, RP time series)	epoch photometry (G, BP, RP time series)	epoch photometry (G, BP, RP time series)
vari_epoch_radial_velocity	rv_obs_time			
vari_epoch_radial_velocity	radial_velocity			
vari_epoch_radial_velocity	radial_velocity_error			

(a)

	Variability types			
gaiadr3. tables	**rotation modulation**	**MS oscillator**	**short timescale**	**long period**
gaia_source	l	l	l	l
gaia_source	b	b	b	b
gaia_source	parallax	parallax	parallax	parallax
vari_summary	median_mag_g_fov	median_mag_g_fov	median_mag_g_fov	median_mag_g_fov
vari_summary	median_mag_bp	median_mag_bp	median_mag_bp	median_mag_bp
vari_summary	median_mag_rp	median_mag_rp	median_mag_rp	median_mag_rp
astrophysical_parameters	ag_gspphot	ag_gspphot	ag_gspphot	ag_gspphot
astrophysical_parameters		mg_gspphot		
astrophysical_parameters		vsini_esphs		
vari_type	source_id	source_id	source_id	source_id
vari_type	best_rotation_period	frequency1	frequency	frequency
vari_type	max_activity_index_g	amplitude_g_freq1	amplitude_estimate	amplitude
vari_type	segments_rotation_period			
vari_type	segments_start_time			
vari_type	segments_end_time			
datalink	epoch photometry (G, BP, RP time series)	epoch photometry (G, BP, RP time series)	epoch photometry (G, BP, RP time series)	epoch photometry (G, BP, RP time series)

(b)

Table 3.2: Astrometric, photometric, spectroscopic and astrophysical parameters for each GDR3 variability class SOS module in the PLATO Input Catalogue.

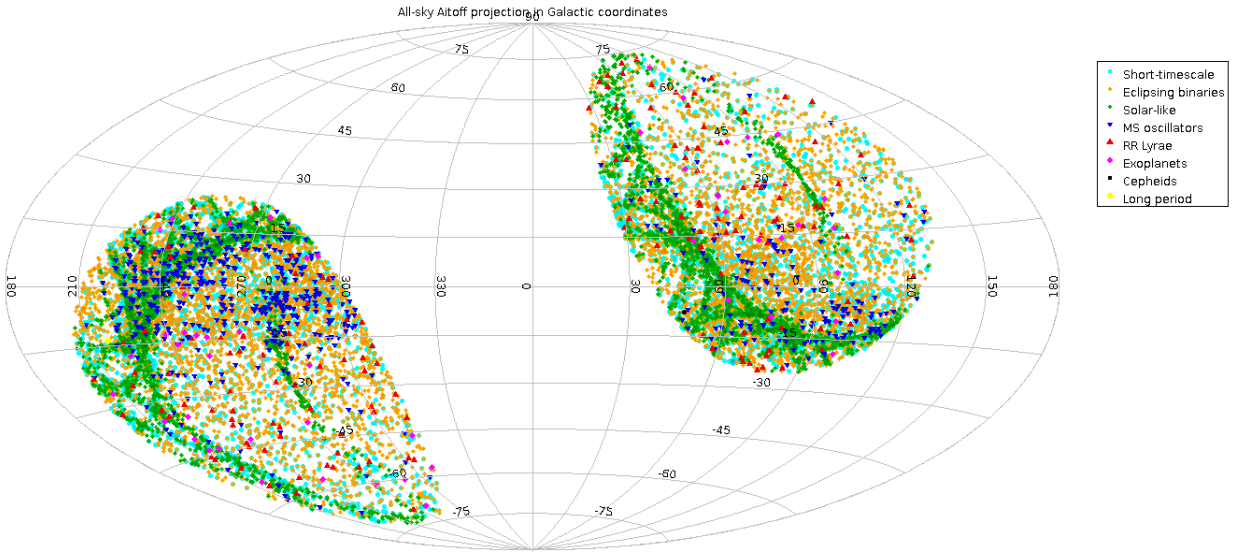

Figure 3.1: All-sky distribution of the variable sources in Aitoff projection and Galactic coordinates

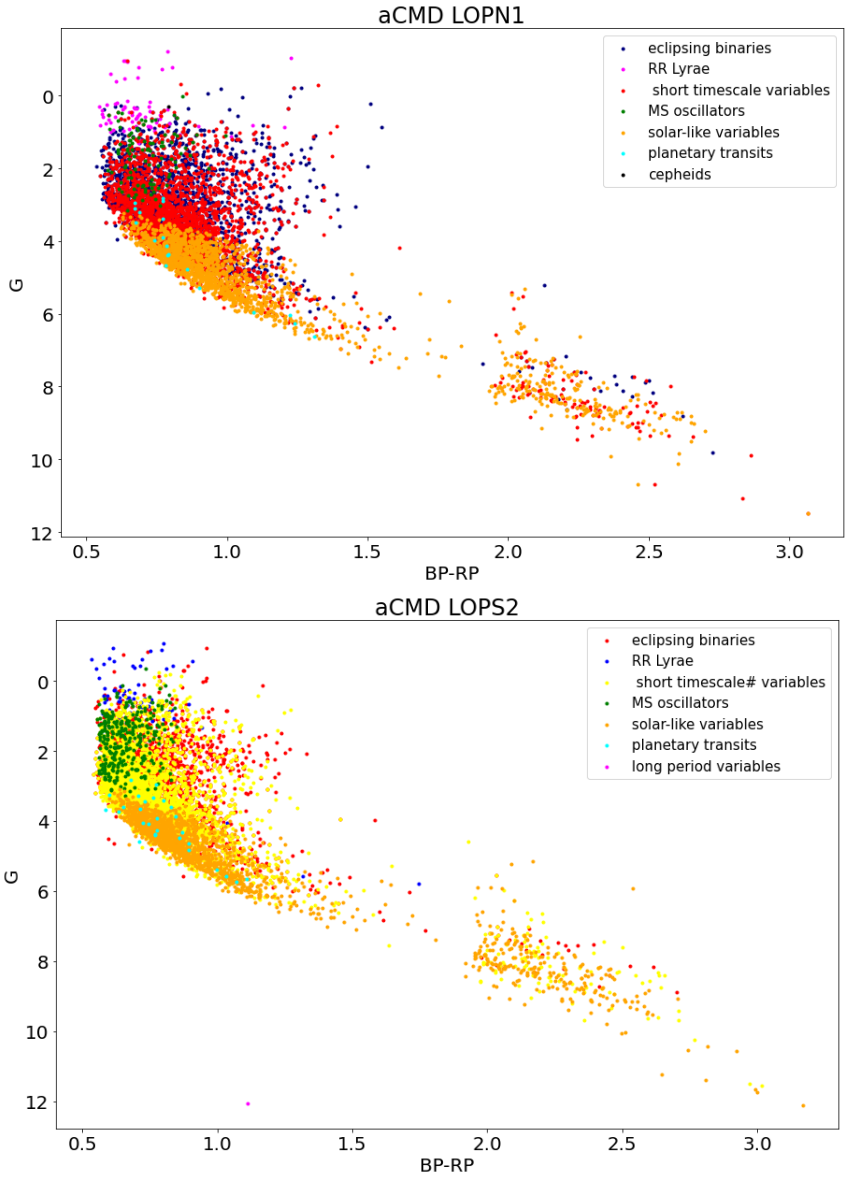

Figure 3.2: Dereddened absolute Color-Magnitude diagrams for both PLATO LOP fields

3.2 RR Lyrae

RR Lyrae stars are a class of pulsating stars known to be excellent distance indicators due to the strong correlation between their absolute magnitude and metallicity, and therefore are used as standard candles for measuring (extra-)galactic distances. They are also regarded as tracers of the chemical and dynamical properties of the oldest observable population of stars, and are typically low mass (M $\approx$ 0.6-0.8 $M_{\odot}$), old (ages $>$ 9-10 Gyr) and metal-poor stars whose surface expands and contracts regularly with periods shorter than a day (Clementini, G. et al. 2022).

RR Lyrae stars can be subclassified into RRab, RRc and RRd depending on their pulsation mode, respectively called fundamental, radial first overtone and double mode (the latter is given by the superposition of the other two ones excited simultaneously).

The ab-type RR Lyrae stars oscillate with periods typically between about 0.42 d and 1 d, their light curves look asymmetrical and sawtooth-shaped and present a variation in brightness of up to one magnitude in the *Gaia* visual G band, while c-type RR Lyrae stars have periods between about 0.2 d and 0.42 d, symmetric and almost sinusoidal light curves and brightness variations of up to about half a magnitude in the visual band.

The PLATO Input Catalogue features 3 RRc stars and 81 RRab stars in the northern outer LOP field, and one RRd star, 8 RRc stars and 69 RRab stars in the southern outer LOP field. In fig. 3.3 the sky map distribution of these periodic pulsating sources can be observed, while fig. 3.4 displays the absolute colour-magnitude diagram corrected for extinction for the RR Lyrae stars of both galactic emispheres. Fig. 3.5 shows the P-A diagram of the pulsation period and the peak to peak amplitude of the light variation in the G band for the total considered sample of RR Lyrae stars, where the sources have been colour-coded according to their metallicity; it appears that the sources with a longer period present lower values of metal abundance. From figure 3.6 (top) it appears that the mean of the magnitude skewness distribution is negative, as it is to be expected for a sample mostly composed of ab-type RR Lyrae stars, whose lightcurves are asymmetrical. The periodic pulsating nature of RR Lyrae can be inferred also from 3.6 (bottom), that shows the ratio of the two bands variances to

be almost constant as a function of the median magnitude per FoV in the G band, with an abrupt increase towards fainter magnitudes probably caused by a noise saturation

The lightcurves of two arbitrary RR Lyrae stars from our sample are collected in figures 3.7 and 3.8, where the typical saw-tooth shape of the RRab class and sinusoidal shape of the RRc class can be respectively observed. The radial velocity time series of the sources RRab Gaia DR3 2926381228470699392 and RRc Gaia DR3 1956531880222667904 are displayed in figures 3.9 and 3.10.

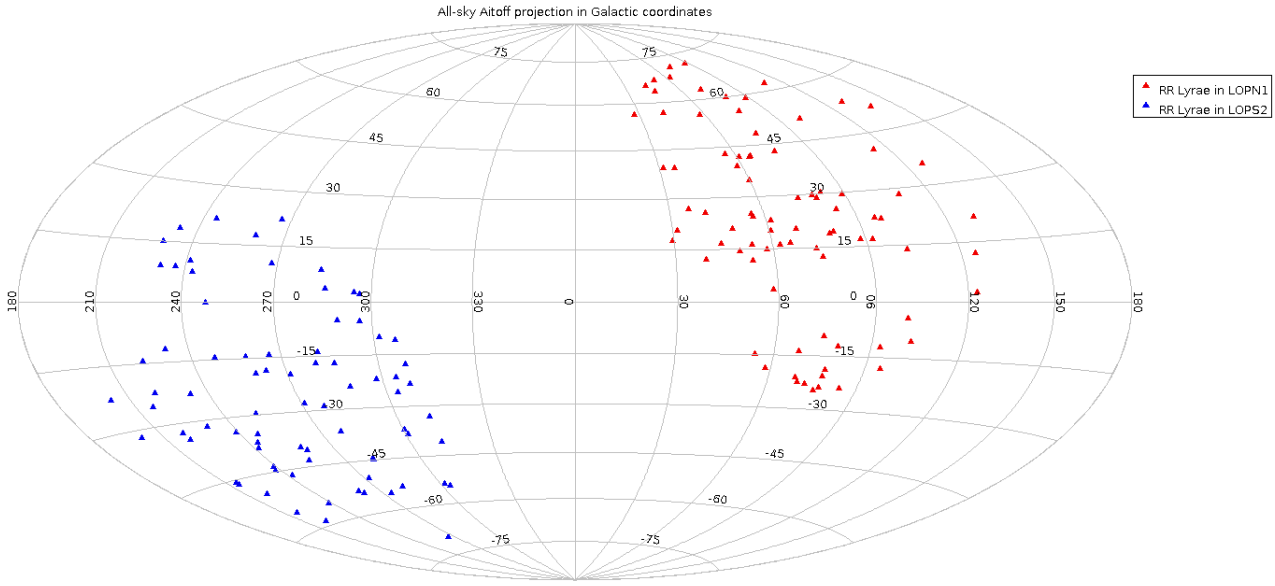

Figure 3.3: Sky map of RR Lyrae stars in Galactic coordinates

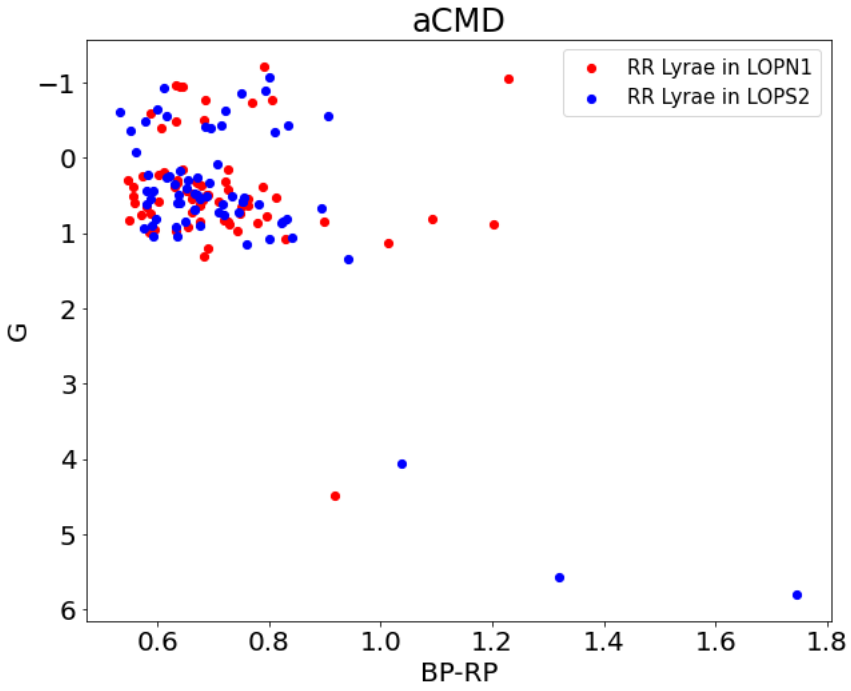

Figure 3.4: Absolute CMD corrected for extinction for the total RR Lyrae sample in PIC

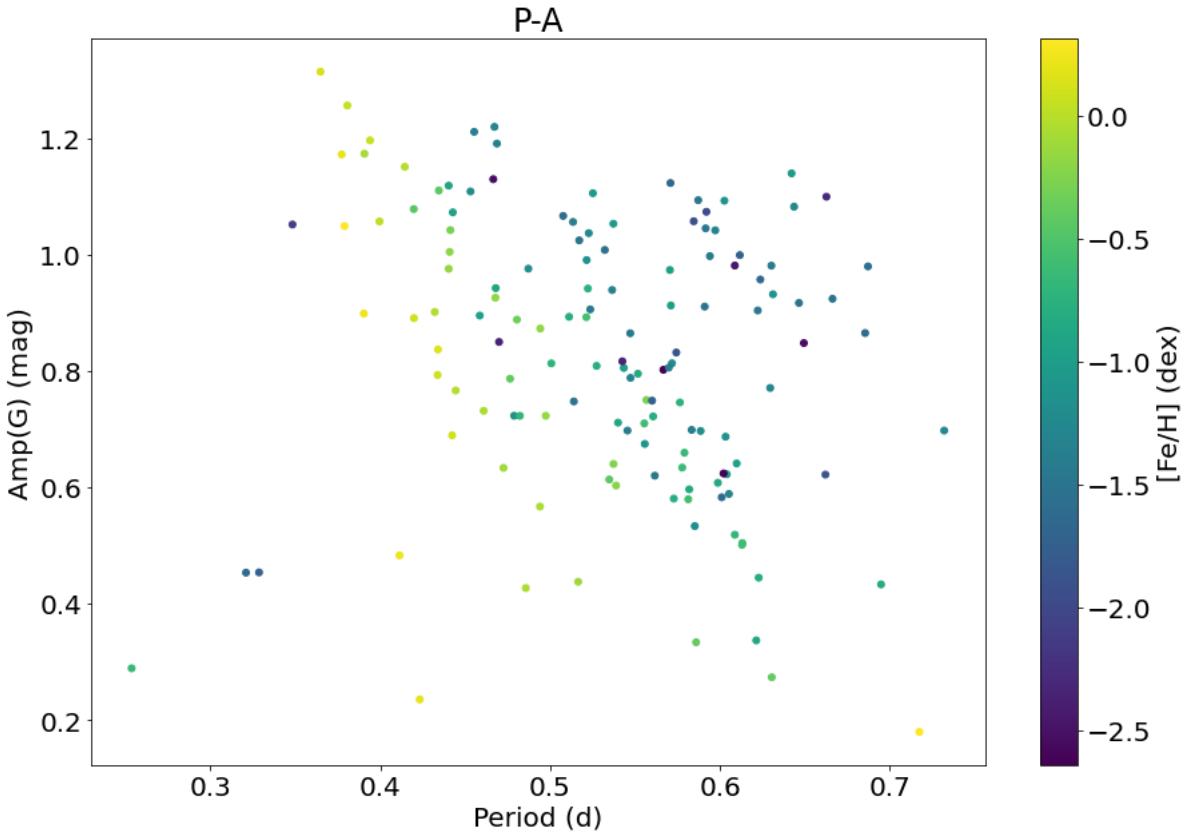

Figure 3.5: Period - Amplitude diagram for RR Lyrae stars colour-coded according to their metallicity

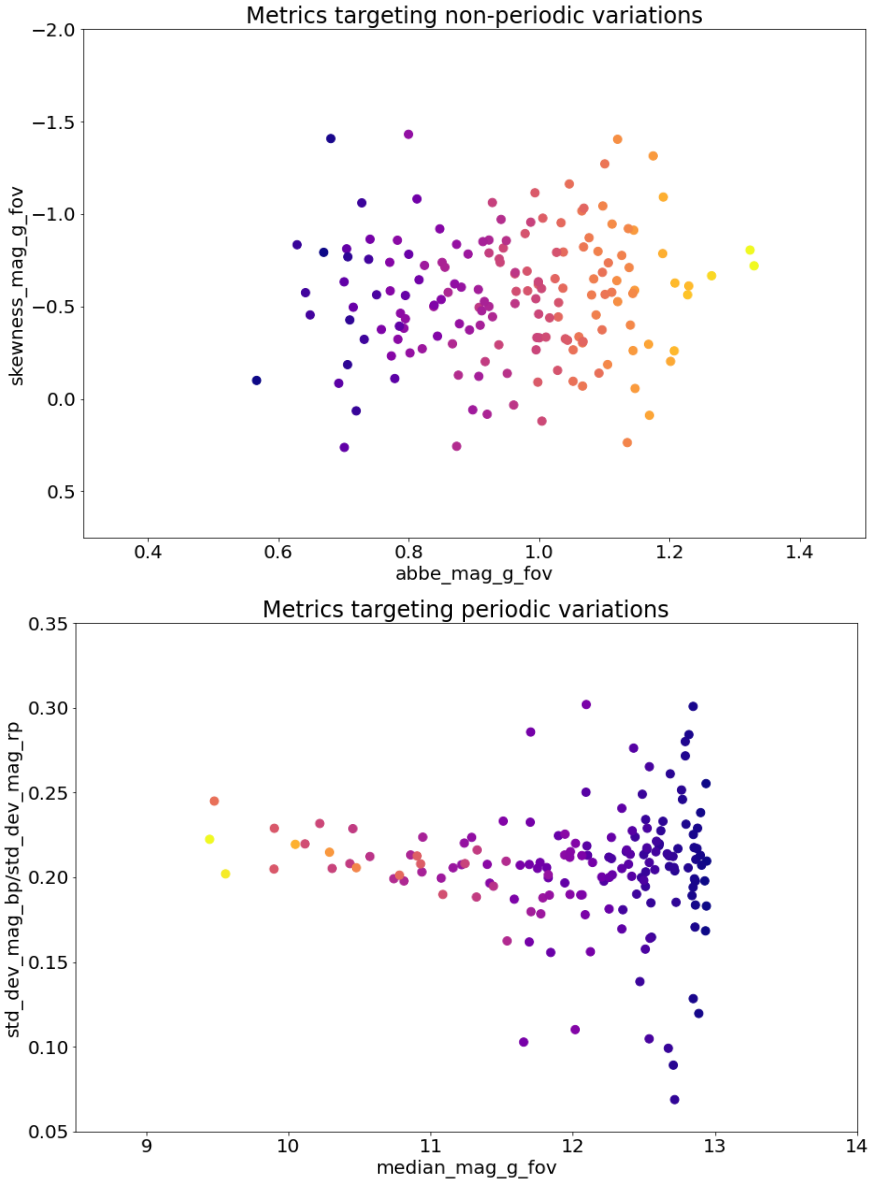

Figure 3.6: Metrics targeting non-periodic (top) and periodic (bottom) variations

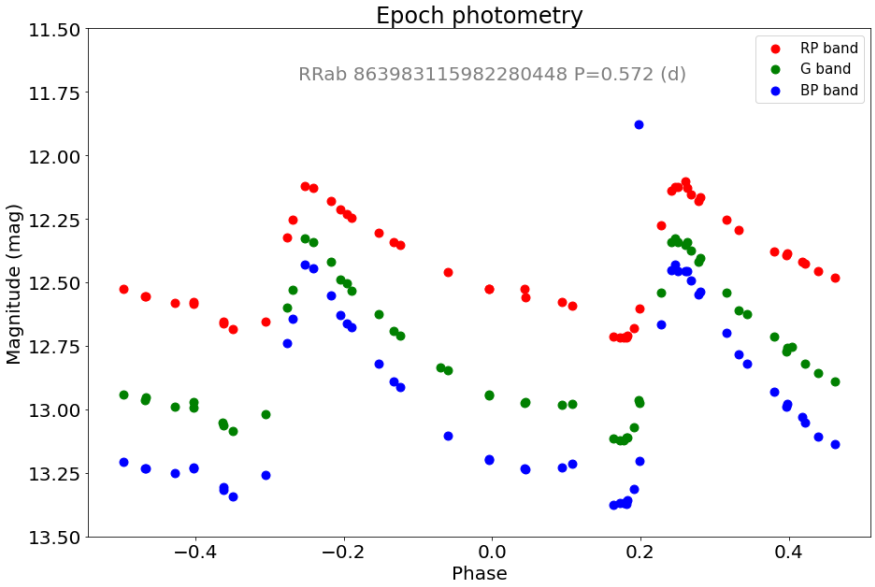

Figure 3.7: Epoch photometry of the ab-type RR Lyrae Gaia DR3 863983115982280448 in the G, G_{BP} and G_{RP} bands in the phase domain.

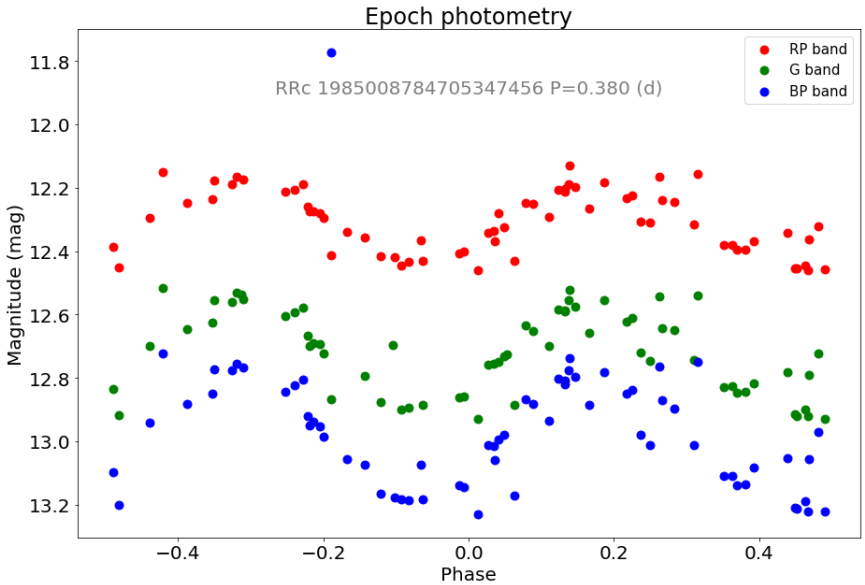

Figure 3.8: Epoch photometry of the c-type RR Lyrae Gaia DR3 1985008784705347456 in the G, G_{BP} and G_{RP} bands in the phase domain.

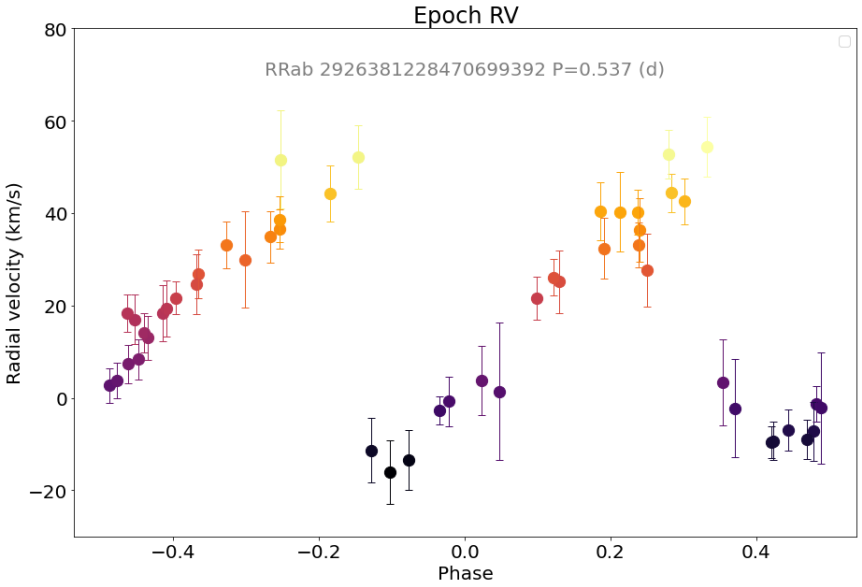

Figure 3.9: Epoch radial velocity of the ab-type RR Lyrae Gaia DR3 2926381228470699392 in the phase domain.

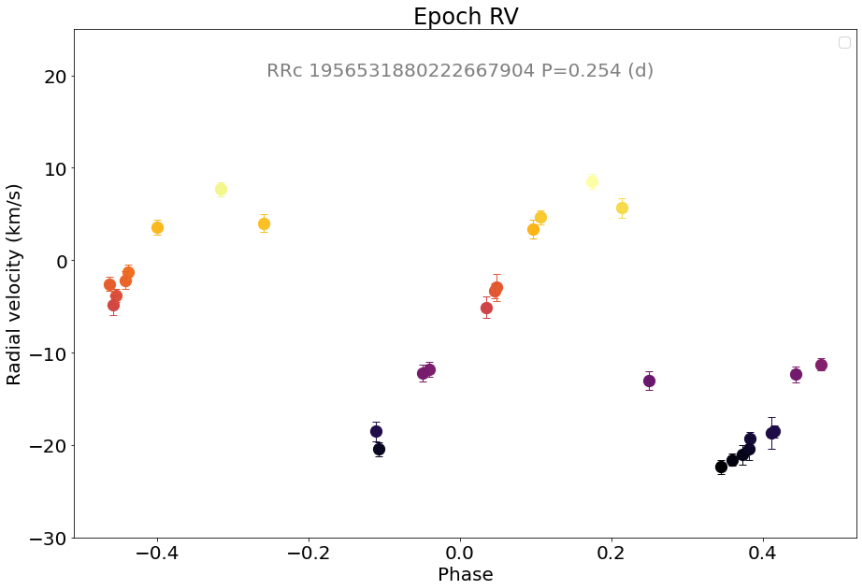

Figure 3.10: Epoch radial velocity of the c-type RR Lyrae Gaia DR3 1956531880222667904 in the phase domain.

3.3 Solar-like variables

For solar-like variable stars (Distefano, E. et al. 2022), the flux variability is induced by the presence and the evolution of magnetically active regions (MARs), such as dark spots and bright faculae. These magnetically active stars present a selection of variability phenomena whose time-scales can range between few minutes, as in the case of flare events, to years, as in the case of the periodic 11-yrs cycle observed in the Sun.
At an intermediate time-scale, solar-like stars' light curves display a rotational modulation signal, which is a quasi-periodic flux variation induced by the stellar rotation that modulates the visibility of MARs over the stellar disk.

The galactic distribution of these variable sources as they are collected in the PLATO Input Catalogue is shown in fig. 3.11, while fig. 3.12 displays their absolute CMD corrected for extinction.

The photometric amplitude A of the rotational modulation signal can be regarded as a proxy of the stellar magnetic activity level, which increases towards shorter rotation periods together with the MARs lifetime; moreover from the period of the rotational modulation signal the stellar rotation period can be inferred. The relationship between A and P can be observed in the density map reported in fig. 3.13, which shows as expected from the literature the presence of three families of rotating stars, classified as Low-Amplitude-Slow-Rotators (LASR), Low-Amplitude-Fast-Rotators (LAFR), and High-Amplitude-Rotators (HAR).
The rotational modulation signal looses coherence and stability across the full Gaia photometric time-series because of the intrinsic evolution of MARs and can be detected only in shorter sub-series, whose duration is comparable with the spots life-time. Therefore when analyzing epoch photometry it is necessary to perform a segmentation of the time-series, where each segment presents a significant period according to which the light curve can be folded. This can be observed in fig. 3.14, where the light curve of the solar-like star Gaia DR3 3934503103368181 is displayed.

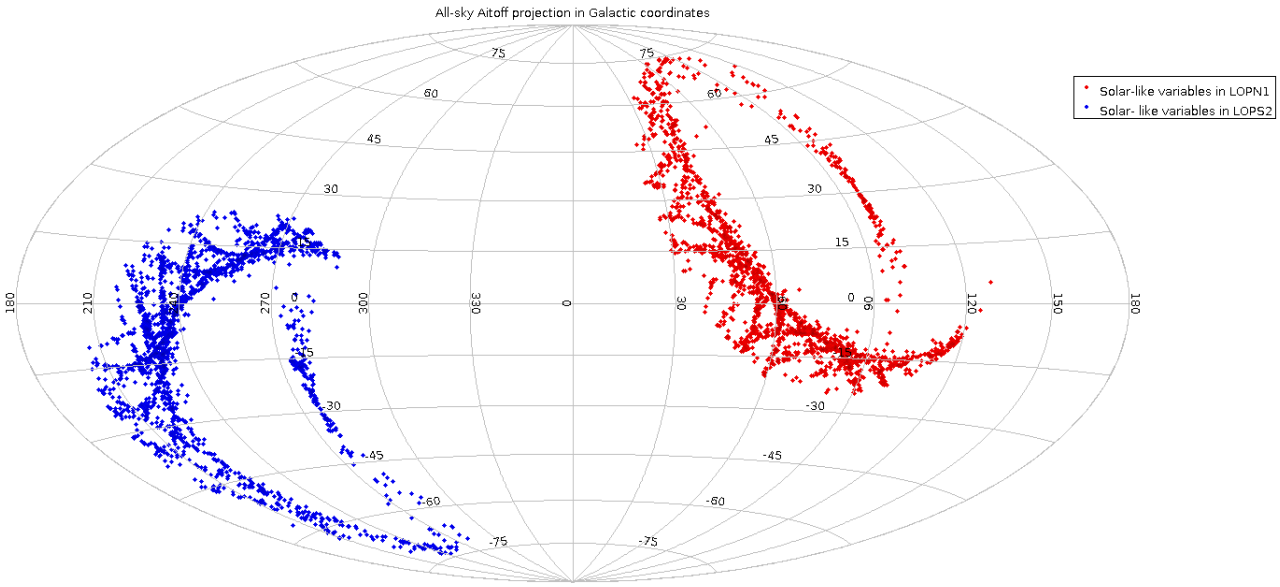

Figure 3.11: Sky map of solar-like variable stars in Galactic coordinates

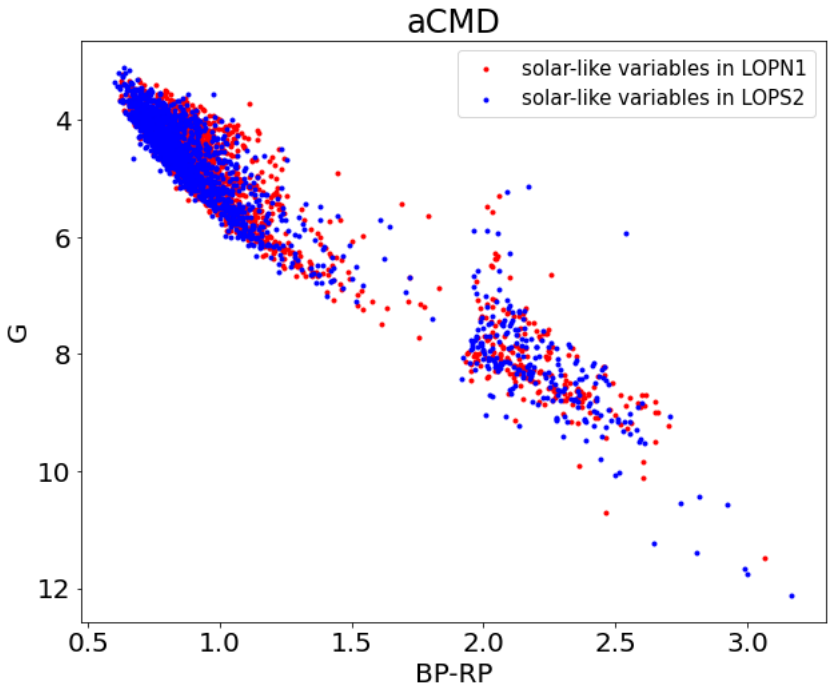

Figure 3.12: Absolute CMD corrected for extinction for the total sample of solar-like variables in PIC

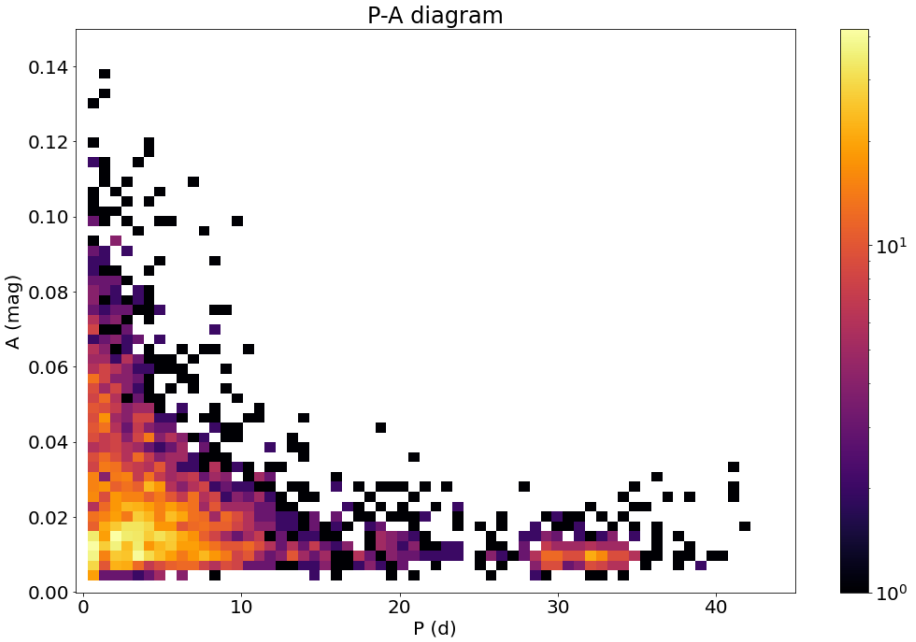

Figure 3.13: Period-Amplitude diagram for the total sample of solar-like variables in PIC

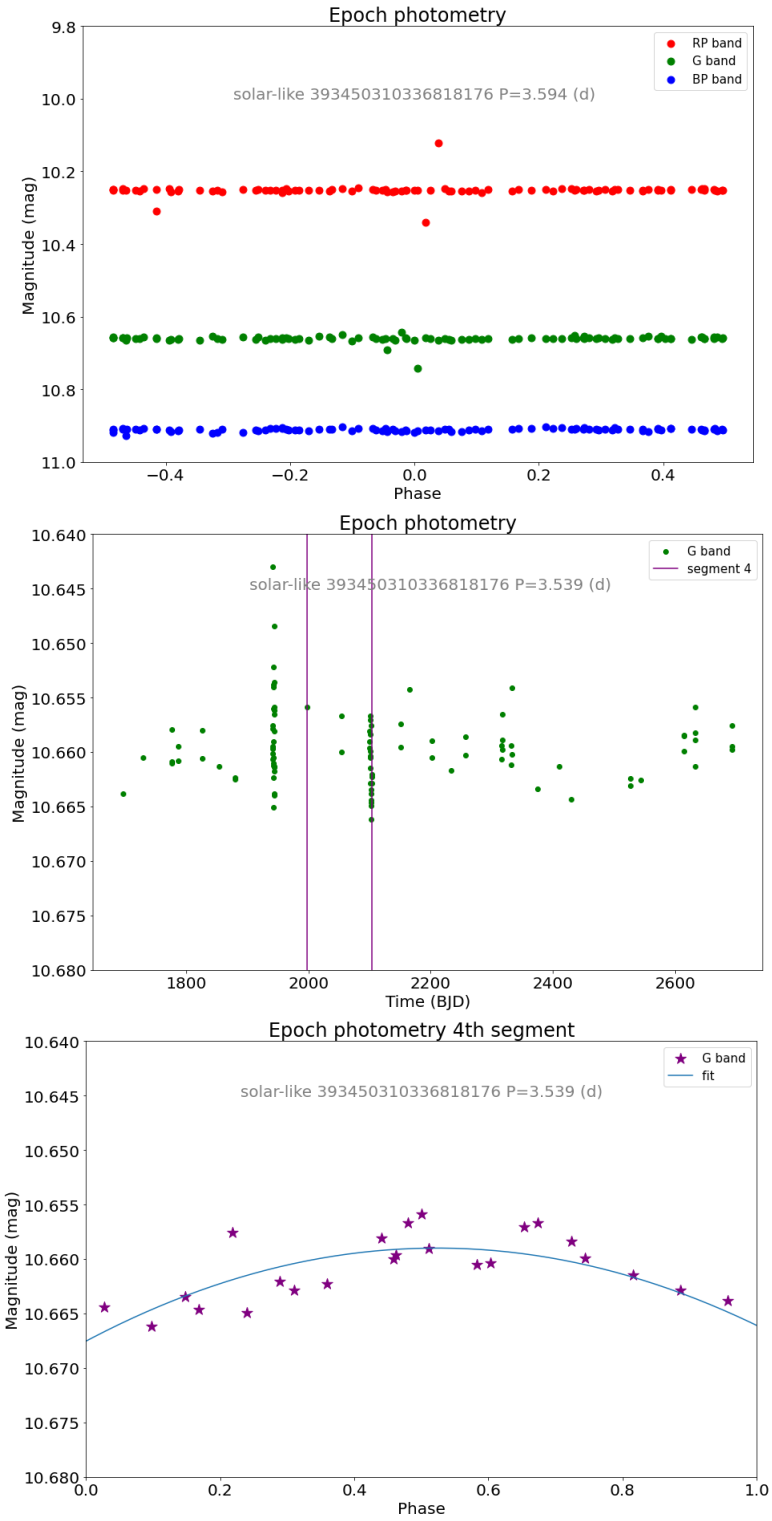

Figure 3.14: Top panel: full G, G_{BP} and G_{RP} time-series for the star Gaia DR3 393450310336818176 folded over the best rotation period P = 3.594 d. Middle panel: full G time-series, where the purple vertical lines enclose the fourth segment. Bottom panel: fourth sub-series folded according to the segment period P = 3.539 d and fitted by a sinusoidal curve.

3.4 Main Sequence oscillators

This sample of variable sources collected in the PLATO Input Catalogue include intermediate-to-high mass upper Main Sequence pulsators of spectral types early-F and hotter; among them SX Phoenicis, γ Doradus and δ Scuti stars can be distinguished, the latter being the most populated variability class.

These non-radial oscillators are often multi-periodic, display very low amplitudes and typically a significant frequency peak can be observed in the Fourier spectrum of their Gaia light curve, associated to a dominant oscillation mode (Gaia Collaboration, De Ridder, J., et al. 2022).

The sky map distribution of the considered sample of upper-MS oscillators is reported in figure 3.15; having convective cores, they occupy the so-called instability strips on the Hertzsprung-Russell (HR) diagram, shown in figure 3.16.

In fig. 3.17 and 3.18 the distribution of the photometric amplitude in the G-band as a function of the primary frequency, and the histogram of the primary frequency can be observed respectively.

From the literature (Gaia Collaboration, De Ridder, J., et al. 2022) δ Scuti stars are known to exhibit an empirical relation between their period and their luminosity: the period- Wesenheit G index diagram for our sample of stars is reported in figure 3.19, which shows two main clusters of pulsators presenting different oscillation regimes. The difference between fast rotating pulsators and slow-to-moderate pulsators arises from the physics of their internal rotation and core convection.

Moreover, from the photometric G-band amplitude-projected rotational velocity plot displayed in fig. 3.20 it can be observed that stellar rotation attenuates the amplitude of the dominant oscillation mode of δ Sct stars, as expected: indeed even from the reduced available sample of stars provided with rotational velocity measurements, it appears that high amplitude sources tend to rotate slower, while the oscillation amplitude decreases for increasing rotational velocities.

The full time-series in the G, G_{BP} and G_{RP} bands for the star Gaia DR3 39332606552108761

and the phase diagram for the same source folded according to its primary frequency are displayed in figure 3.21.

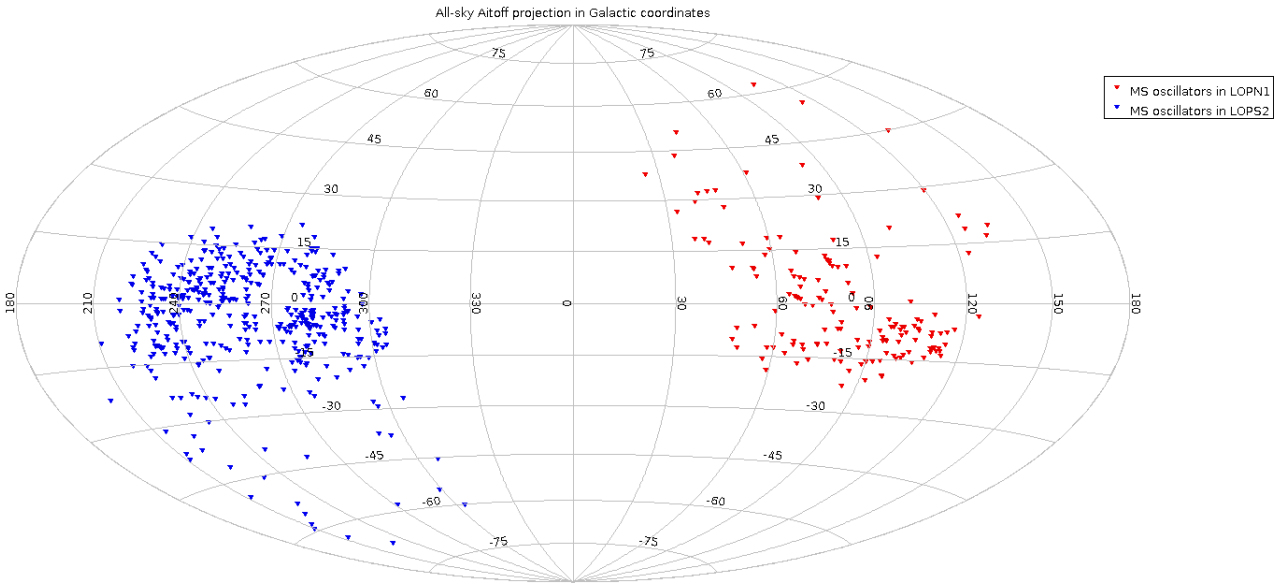

Figure 3.15: Sky map of Main Sequence oscillators in Galactic coordinates

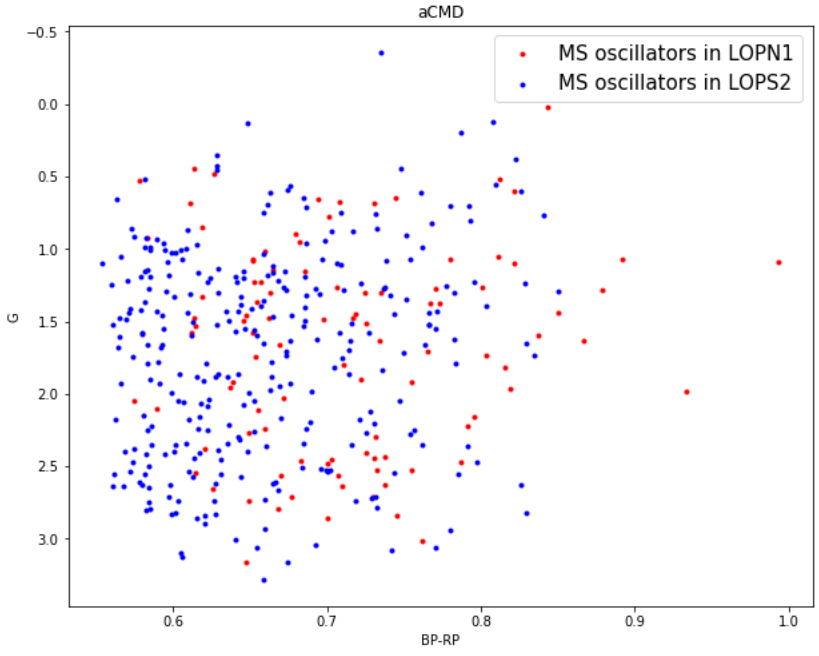

Figure 3.16: Absolute CMD corrected for extinction for the total sample of MS oscillators in PIC

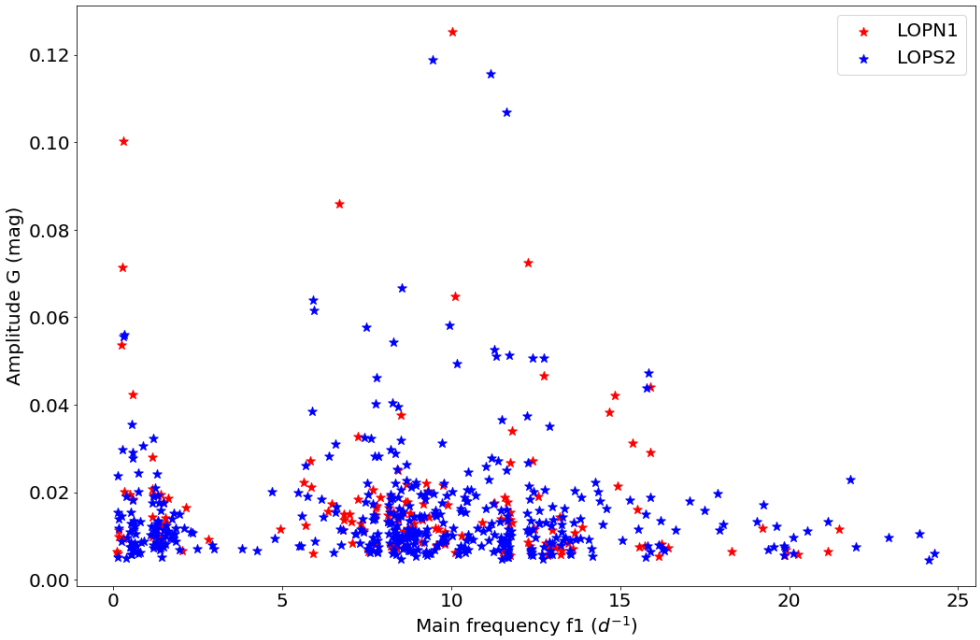

Figure 3.17: G-band amplitude-main frequency distribution

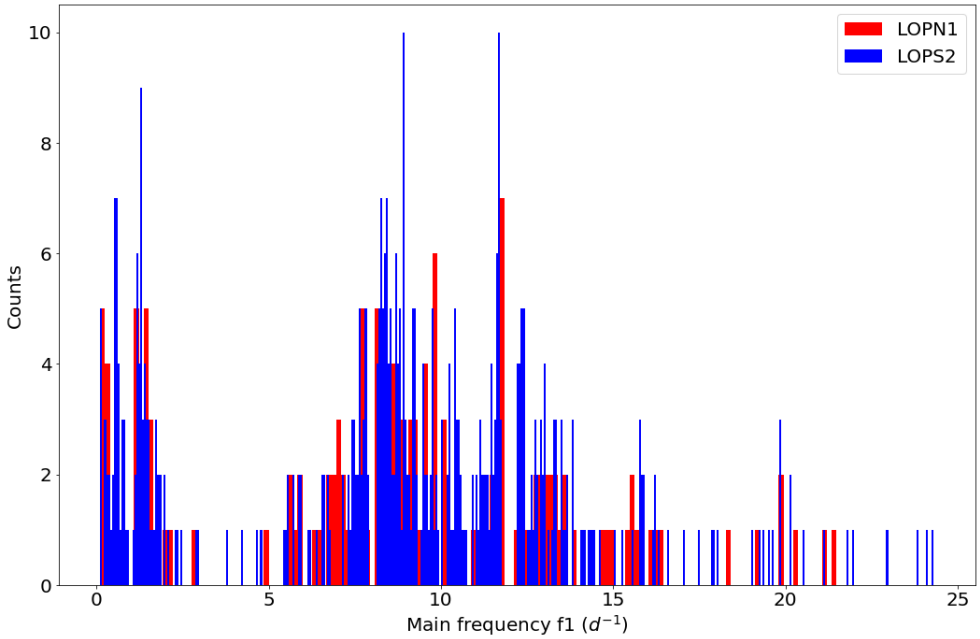

Figure 3.18: Histogram of the primary frequency for the upper-MS pulsators of both LOP fields.

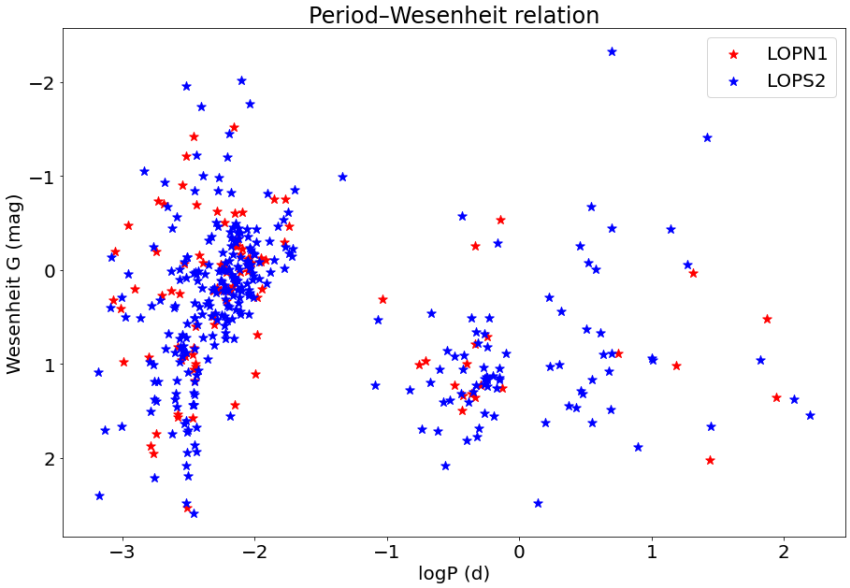

Figure 3.19: Period-Wesenheit G diagram for the upper-MS pulsators of both LOP fields.

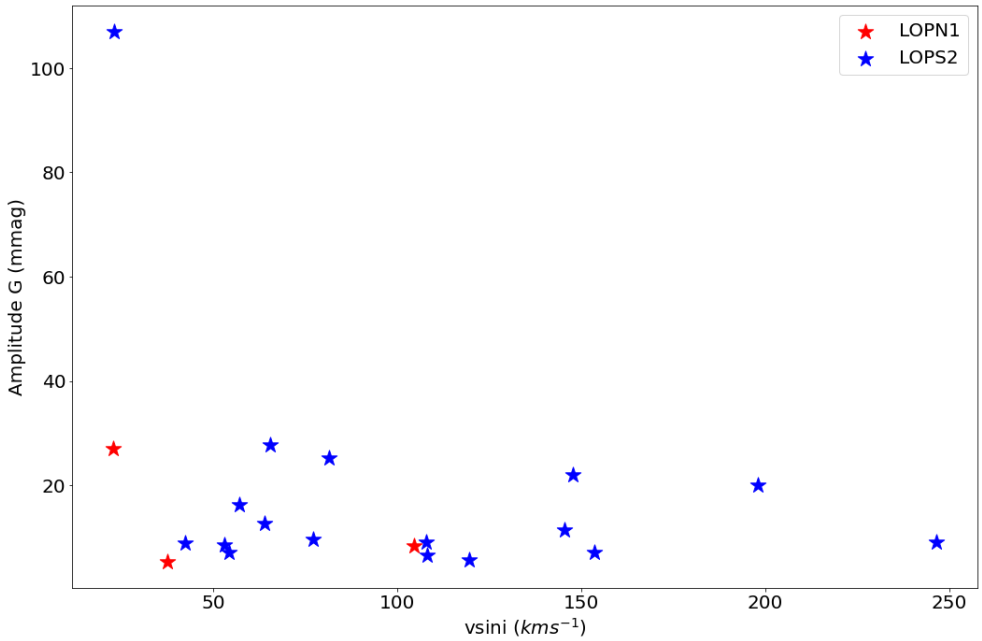

Figure 3.20: Photometric amplitude A in the Gaia G-band as a function of the projected rotational velocity for a sample of δ Sct stars.

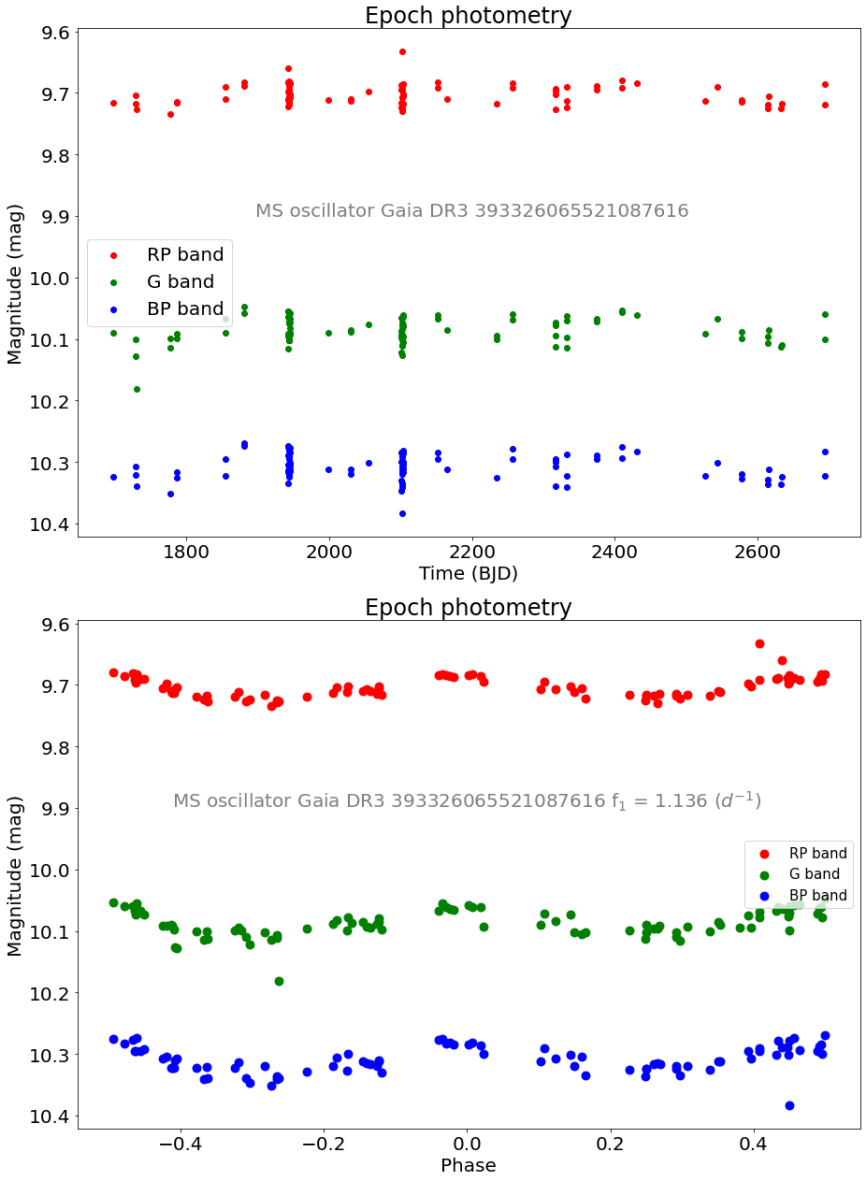

Figure 3.21: Top: photometric time series for the pre MS oscillator Gaia DR3 3933260655210876 16 in the G, G_{BP} and G_{RP} bands. Bottom: phase diagram for the same source folded according to its primary frequency.

3.5 Planetary transits

This class of photometric variables includes Main Sequence F-type stars displaying signatures of exoplanetary transits. Thanks to the high spatial resolution and its multi-epoch photometry, and despite its sparse and low-cadence observations, Gaia can identify false-positive candidates and confirm true detections of transiting planets from TESS exoplanetary candidates. Indeed Panahi et al. 2022 have confirmed the mission's very first two new Hot-Jupiters via RV follow up observations, Gaia-1b and Gaia-2b.

The Gaia DR3 planetary transits SOS module is composed of 173 known exoplanets with visible transits in the photometry of Gaia and 41 new candidates; the sample has been obtained through a a dedicated implementation of the BLS algorithm with the aim of searching for significant transit-like signals in the candidates light curves in the Full-Frame Image (FFI) photometry of TESS.

The known confirmed and the candidate transiting extra-solar planet hosts that are included in the PLATO Input Catalogue are collected in tables 3.3 and 3.4 respectively for the two Long-duration Observation Phase pointing fields. Specifically 3 out of 21 are candidate exoplanetary hosts in the northern LOP field, while 7 out of 31 are the candidates in the southern LOP field.

The sky distribution of the PIC planetary transit events (whether alleged or confirmed) in Galactic coordinates and in Aitoff projection is shown in figure 3.22; their observational Hertzsprung-Russell diagram is reported in figure 3.23.

Figure 3.24 displays the lightcurve of the confirmed exoplanetary host KELT-16 (Gaia DR3 *source_id* 1864885215233116032), a yellow-white star of spectral class F7V closely orbited by a hot Jupiter; in figure 3.25 instead the lightcurve of the candidate exoplanetary host TYC 3970-844-1 (Gaia DR3 *source_id* 2177849036734191744) is reported.

Gaia DR3 *source_id*	Main ID	Spectral type	Exoplanet	References
1334573817793362560	HAT-P-18	K2V	HAT-P-18 b	1 2 3 4 5
1928431764627661440	BD+37 4734B	G0V	HAT-P-1 b	1 2 3 4 5
1962153854973972096	HAT-P-40	F	HAT-P-40 b	1 2 3 4 5
1316708918505350528	BD+28 2507	G1V	XO-1 b	1 2 3 4 5
1622997463177004928	WISEA J160752.17+574902.9		N/A	1 4 6
1864885215233116032	KELT-16	F7V	KELT-16 b	1 2 3 4 5
2262322556576778752	Qatar-10	F7V	Qatar-10 b	1 2 3 4 5
2244830490514284928	Qatar-1	K	Qatar-1 b	1 2 3 4 5
1424011082893734272	WASP-92	F7	WASP-92 b	1 2 3 4 5
4606030169272920320	HAT-P-5	G1V	HAT-P-5 b	1 2 3 4 5
2177849036734191744	TYC 3970-844-1		N/A	1 2 4 5
4609062308806929152	TYC 2620-648-1	F8	TrES-4 b	1 2 3 4 5
4609131509318715136	1SWASP J175207.01+373246.3	G	TrES-3 b	1 2 3 4 5
2102117871259036672	Kepler-7	G0	Kepler-7 b	1 2 3 4 5
2129256395211984000	BD+47 2846	F6V	HAT-P-7 b	1 2 3 4 5
2141754578242371584	WASP-48	G0IV	WASP-48 b	1 2 3 4 5
1499514786891168640	HAT-P-12	K5	HAT-P-12 b	1 2 3 4 5
4535127268607000320	WISEA J183411.49+220908.4		N/A	1 4 6
1644692064543192704	BD+66 911	K	KELT-23A b	1 2 3 4 5
1827242816201846144	HD 189733	K2V	HD 189733 b	1 2 3 4 5
1587399232335653760	WASP-113	G1	WASP-113 b	1 2 3 4 5

Table 3.3: List of the 21 confirmed and candidate transiting exoplanet hosts in LOPN1.

[1]http://cdsportal.u-strasbg.fr/
[2]http://simbad.u-strasbg.fr/
[3]http://exoplanet.eu/catalog/
[4]https://vizier.cds.unistra.fr/
[5]https://exofop.ipac.caltech.edu/tess/
[6]https://ned.ipac.caltech.edu/

Gaia DR3 *source_id*	Main ID	Spectral type	Exoplanet	References
5345417757181174144	WISEA J114230.50-523738.6		N/A	1 4 6
5608644895310998272	HATS-51	G	HATS-51 b	1 2 3 4 5
5594445630358459648	2MASS J07545687-3221219		N/A	1 4 6
4895643593611507584	WISEA J041929.55-255735.4		N/A	1 4 6
4899428146994060800	HATS-5	K0	HATS-5 b	1 2 3 4 5
4906145613282734208	HATS-30	G1	HATS-30 b	1 2 3 4 5
4677436783705094912	WISEA J043143.94-612309.1		N/A	1 4 6
5565050255701441664	CD-38 3220	F6V	WASP-121 b	1 2 3 4 5
5583523425437258240	WASP-64	G7	WASP-64 b	1 2 3 4 5
5578530470116727936	WISEA J070548.04-351521.8		N/A	1 4 6
3211188618762023424	BD-06 1077	G0	WASP-35 b	1 2 3 4 5
5348534425968598400	TYC 8225-452-1		N/A	1 2 4 5
4851398799032507776	WASP-139	K0	WASP-139 b	1 2 3 4 5
4864759888238232320	WASP-159	F9	WASP-159 b	1 2 3 4 5
4955371367334610048	HD 10069	F6V	WASP-18 b	1 2 3 4 5
2959177048983750016	WASP-61	F7	WASP-61 b	1 2 3 4 5
5656896924435896832	HATS-26	F	HATS-26 b	1 2 3 4 5
5444147952811517696	WASP-66	F4	WASP-66 b	1 2 3 4 5
5557345496687437696	WASP-23	K1V	WASP-23 b	1 2 3 4 5
4746157737910069888	CD-50 714	F9	WASP-117 b	1 2 3 4 5
5086537022856406272	WASP-22	G	WASP-22 b	1 2 3 4 5
5089851638095503616	WASP-78	F8	WASP-78 b	1 2 3 4 5
6386751579018596864	WASP-91	K3	WASP-91 b	1 2 3 4 5
5735158757648658048	UCAC4 384-050987		N/A	1 2 4 5
5262709709389254528	TOI-150	F	TOI-150 b	1 2 3 4 5
5560886336446650240	CD-42 3043	G4	WASP-122 b	1 2 3 4 5
2980392087185289216	WASP-141	F9	WASP-141 b	1 2 3 4 5
5489780919480009472	CD-51 2720	G0	KELT-15 b	1 2 3 4 5
4911563216311083392	CD-56 324	G5	WASP-97 b	1 2 3 4 5
2991284369063612928	WASP-49	G6V	WASP-49 A b	1 2 3 4 5
5723772524469252096	WASP-169	G0	WASP-169 b	1 2 3 4 5

Table 3.4: List of the 31 confirmed and candidate transiting exoplanet hosts in LOPS2.

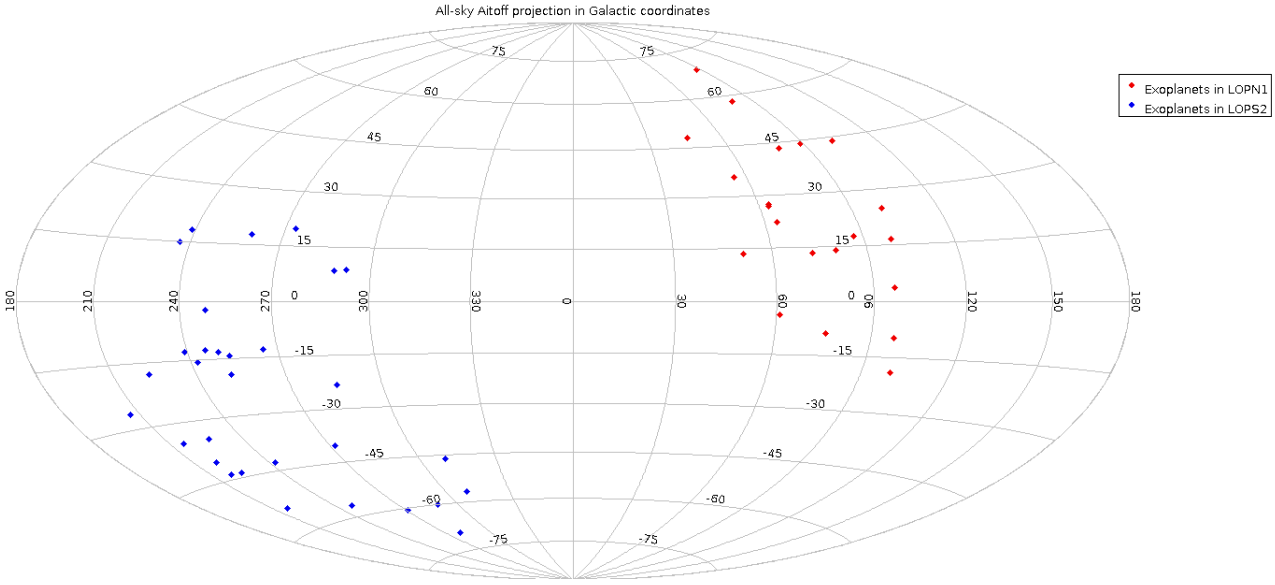

Figure 3.22: Sky map of variable stars showing planetary transits signals in Galactic coordinates

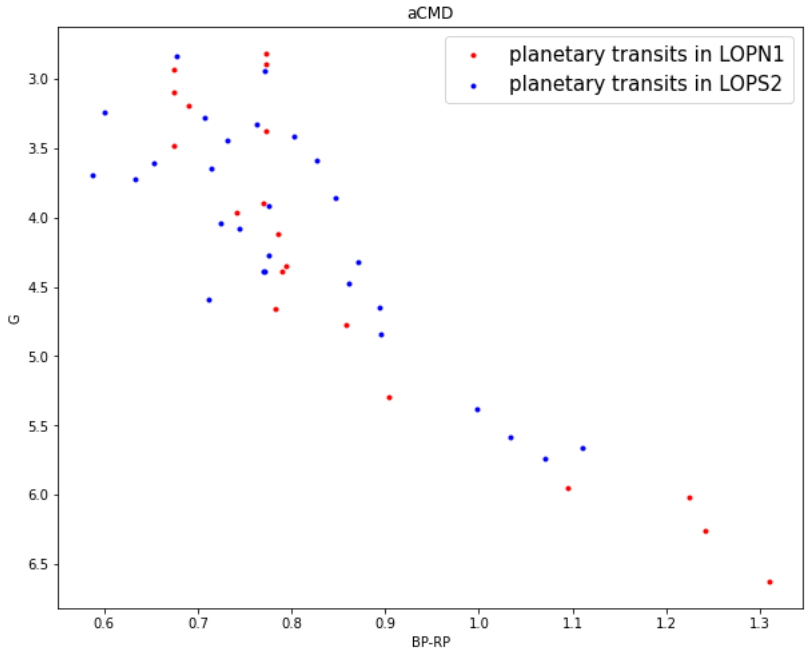

Figure 3.23: Absolute CMD corrected for extinction for the total sample of planet hosts in PIC

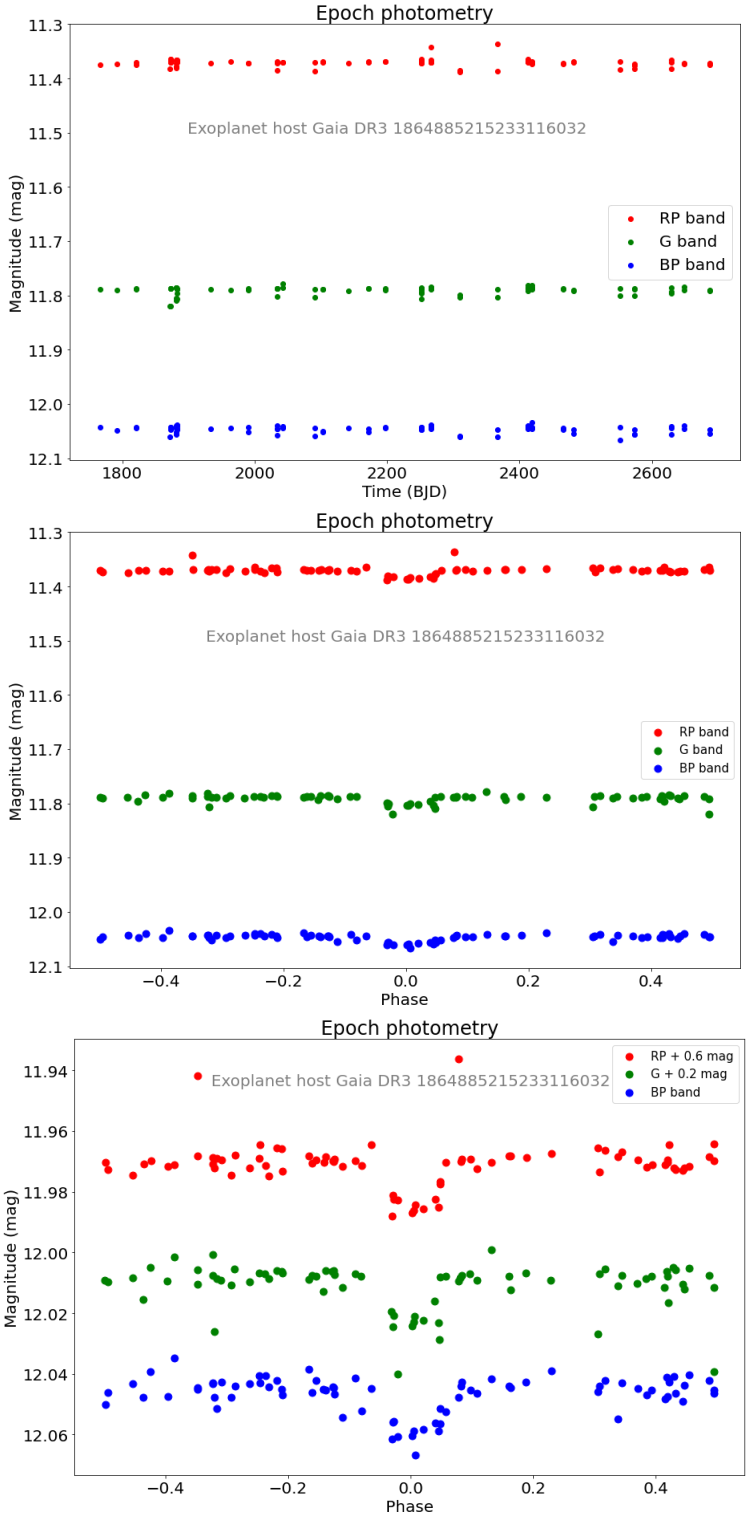

Figure 3.24: Top panel: full time-series in the G, G_{BP} and G_{RP} bands for the extra-solar planet host KELT-16 (Gaia DR3 1864885215233116032). Middle panel: phase-folded light curves according to the transit orbital period P = 0.97 d. Bottom panel: zoom on the phase diagram displaying the transit event in the three photometric bands.

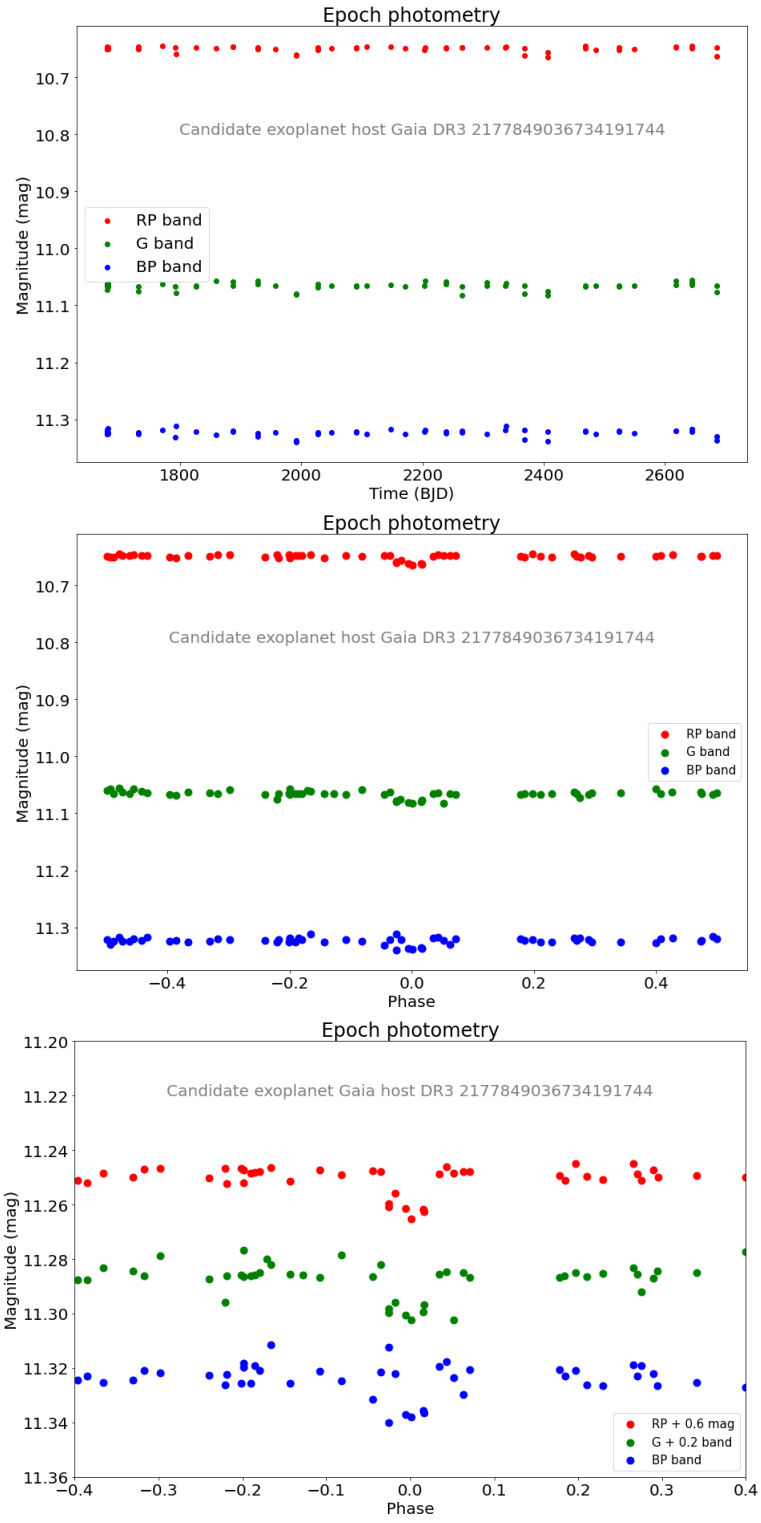

Figure 3.25: Same as figure 3.24 but for the candidate exoplanetary host Gaia DR3 2177849036734191744 (TYC 3970-844-1). The light curves in the middle and bottom panels have been folded according to the period P = 3.81 d.

3.6 Eclipsing binaries

While the majority of stars is in binary systems, only a fraction of them appears to the observer as eclipsing; this family is of capital importance, since eclipsing binaries allow to derive the stars' physical and orbital parameters, play a fundamental role in stellar evolution and their eccentricity can be used as a test for the theory of general relativity. Moreover from variations in the eclipse timings the presence of extra-solar planets can be inferred.
Gaia DR3 Catalogue contains 813687 unique non-single star sources between astrometric, spectroscopic, photometric binaries and higher order stellar systems (Gaia Collaboration, F. Arenou, et al. 2022); moreover it includes the largest collection to date (2184477 sources) of eclipsing binaries (86918 of which provided with orbital solutions), whose brightnesses span from a few magnitudes to 20 mag in the Gaia G-band (Mowlavi et al. 2022).
The PLATO Input Catalogue features Algol (β Persei) type (EA), β Lyrae type (EB), and W Ursae Majoris type (EW) eclipsing binaries, distributed between the northern (2977 sources) and southern (3466 sources) observation fields.

Their distributions in the Aitoff Galactic projection and in the observational Hertzsprung–Russell diagram are shown in figures 3.26 and 3.27 respectively.

It is possible to identify different groups of eclipsing binaries among the sample, from wide (P $>$ 50 d) to tight (P $<$ 10 d) systems, in the orbital period histogram displayed in figure 3.28.

The G, G_{RP} and G_{BP} light curves of the eclipsing binary Gaia DR3 393454948901343360 is shown in figure 3.29, where the gaussian shape of the primary eclipse is clearly visible at phase = 0.2.

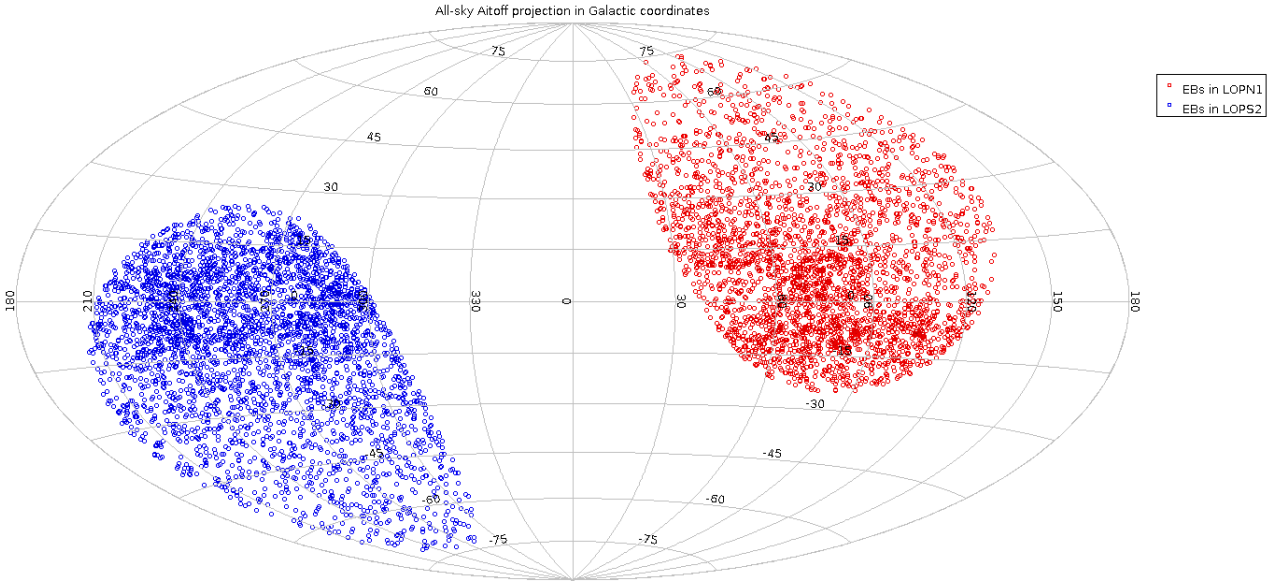

Figure 3.26: Sky map of eclipsing binaries in Galactic coordinates

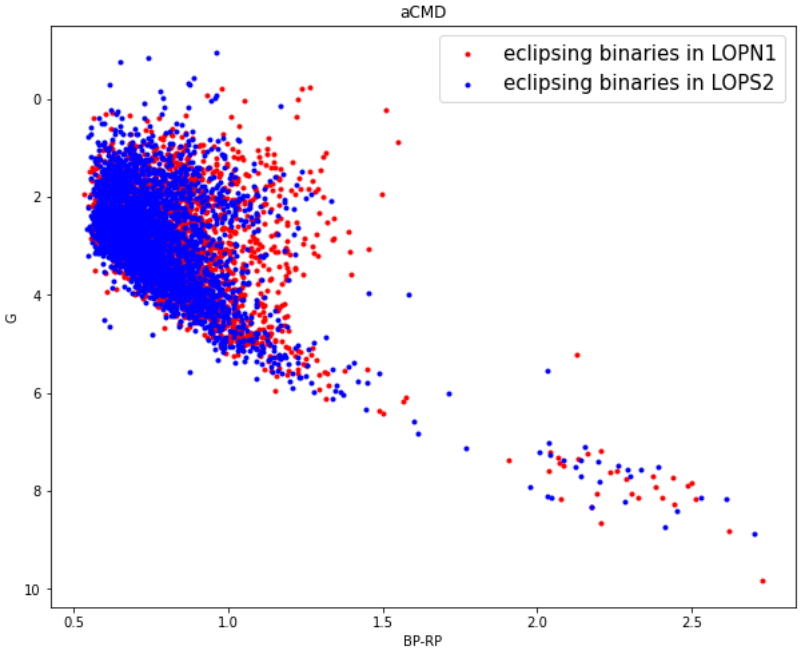

Figure 3.27: Absolute CMD corrected for extinction for the total sample of eclipsing binaries in PIC

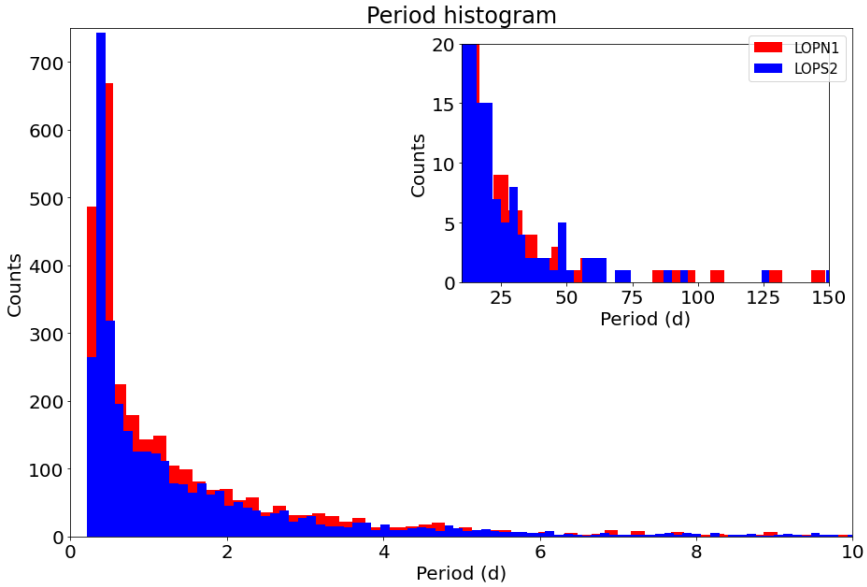

Figure 3.28: Distribution of the orbital periods of the PIC eclipsing binaries.

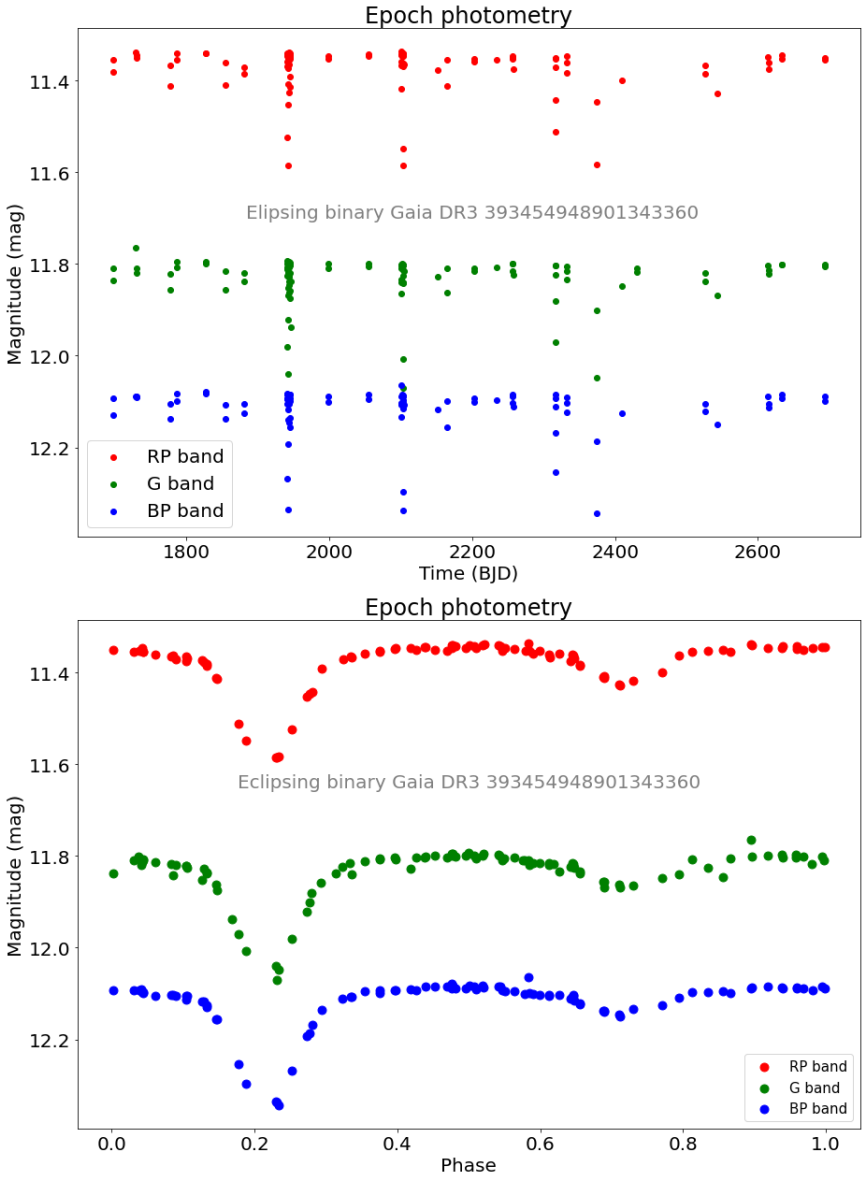

Figure 3.29: Light curve of the eclipsing binary Gaia DR3 3934549489013433 60, in the time domain (top) and folded according to the orbital period P = 1.72 d (bottom).

3.7 Short timescale variables

The PLATO Input Catalogue counts over seven thousands objects that exhibit very fast variability, with periods ranging from 20 minutes to a day [7] and amplitudes ranking from a few millimagnitudes to a few magnitudes. These short-timescale variable sources are classified as EW-type eclipsing binaries, post-common envelope binaries (PCEB), cataclysmic variables (CV), RRab Lyrae stars, solar-like variables (rotational modulation, BY Draconis, RS Canum Venaticorum stars) and Main Sequence oscillators such as δ Scuti stars.

Gaia provides an exceptional opportunity for comprehensive fast-variability studies over the whole sky, thanks to its fast cadence time sampling in G band and its high photometric precision.

Roelens et al. 2018 identified the candidates to be included in the Gaia DR3 *short_timescale* SOS module via variogram analysis; this method quantifies the magnitude variations between photometric measurements as a function of the time lag between them and defines a detection threshold above which the variability is significant enough at time lags shorter than 12 h.

The all-sky map in Aitoff projection and Galactic coordinates of the PLATO Input Catalogue's short timescale variables is shown in figure 3.30, while fig. 3.31 displays the observational Hertzsprung-Russell diagram corrected for extinction. In figures 3.32 and 3.33 the amplitude-frequency plot and the periods distribution can be observed. The lightcurves in time and phase domain of the short-timescale eclipsing binary Gaia DR3 4594961454434214144 are reported in figure 3.34.

[7] Sources with periods between 0.5 and 1 d are considered 'extended' short- timescale variables.

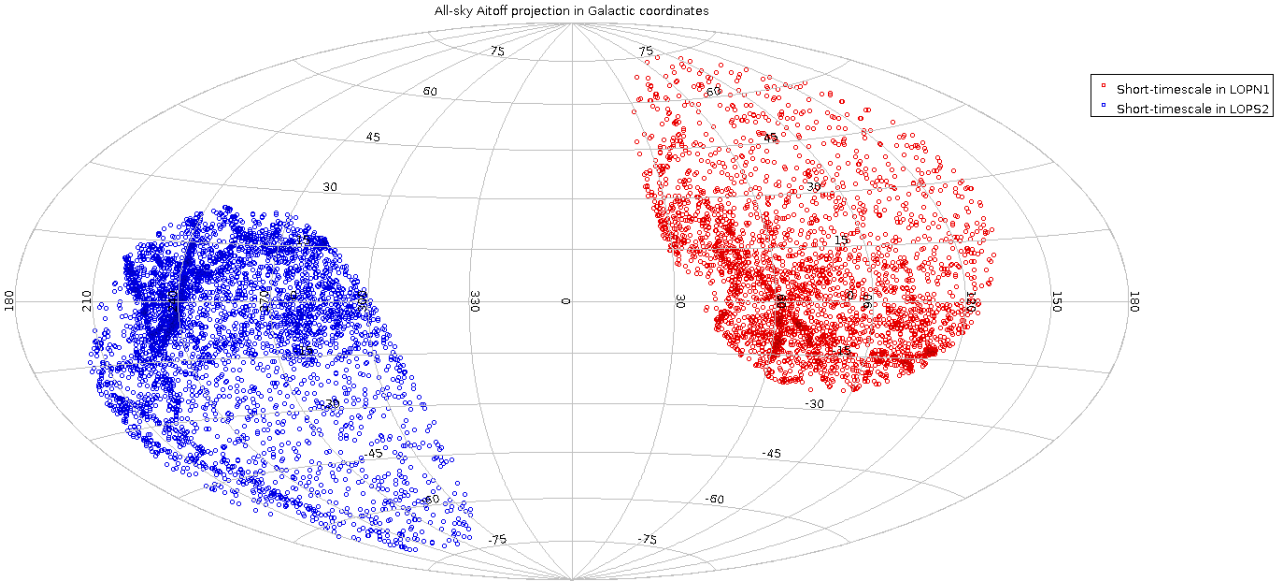

Figure 3.30: Sky map of short-time variables in Galactic coordinates

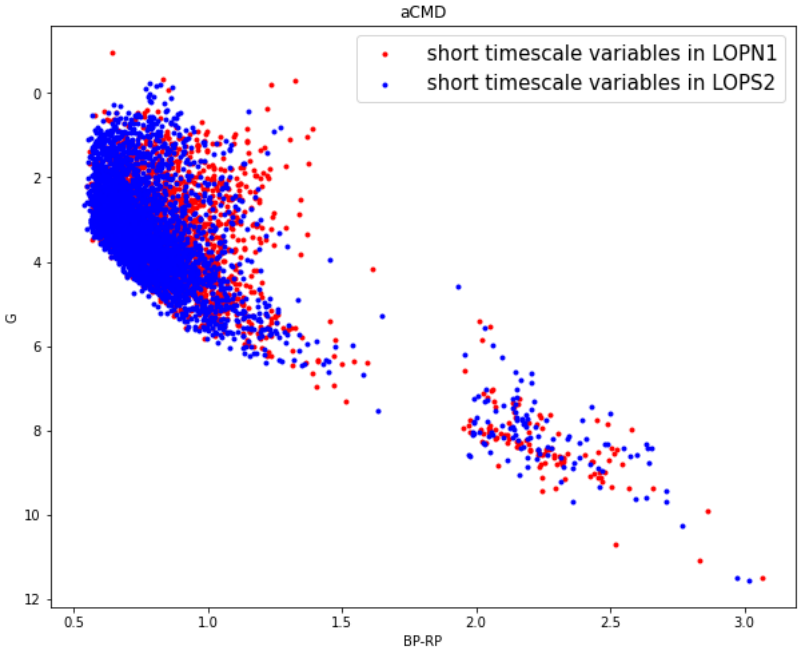

Figure 3.31: Absolute CMD corrected for extinction for the total sample of short timescale variables in PIC

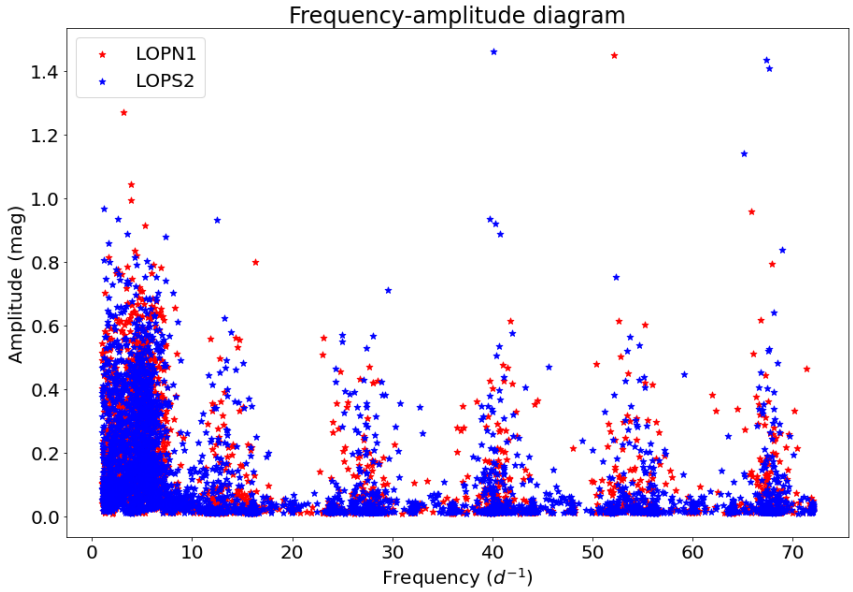

Figure 3.32: Frequency-amplitude distribution for the short-timescale variables in PIC.

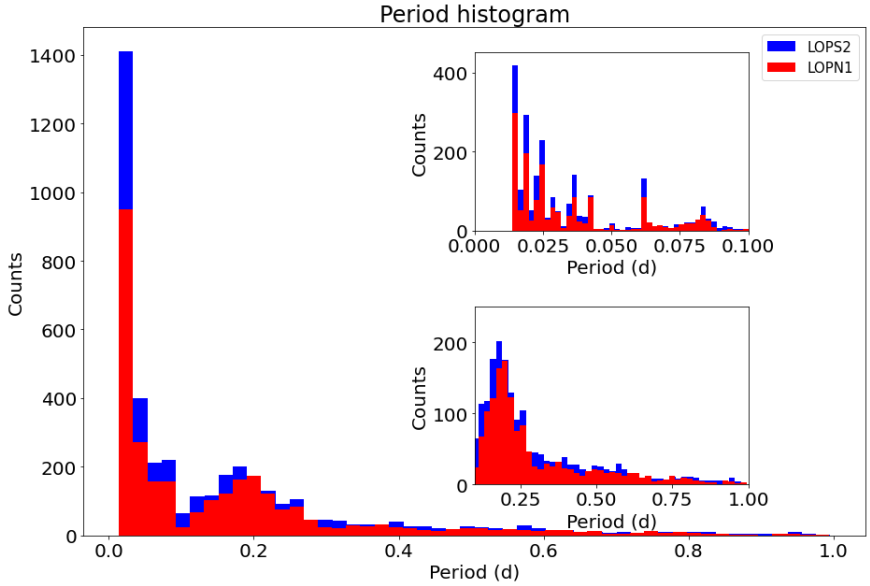

Figure 3.33: Period distribution for the short-timescale variables in PIC.

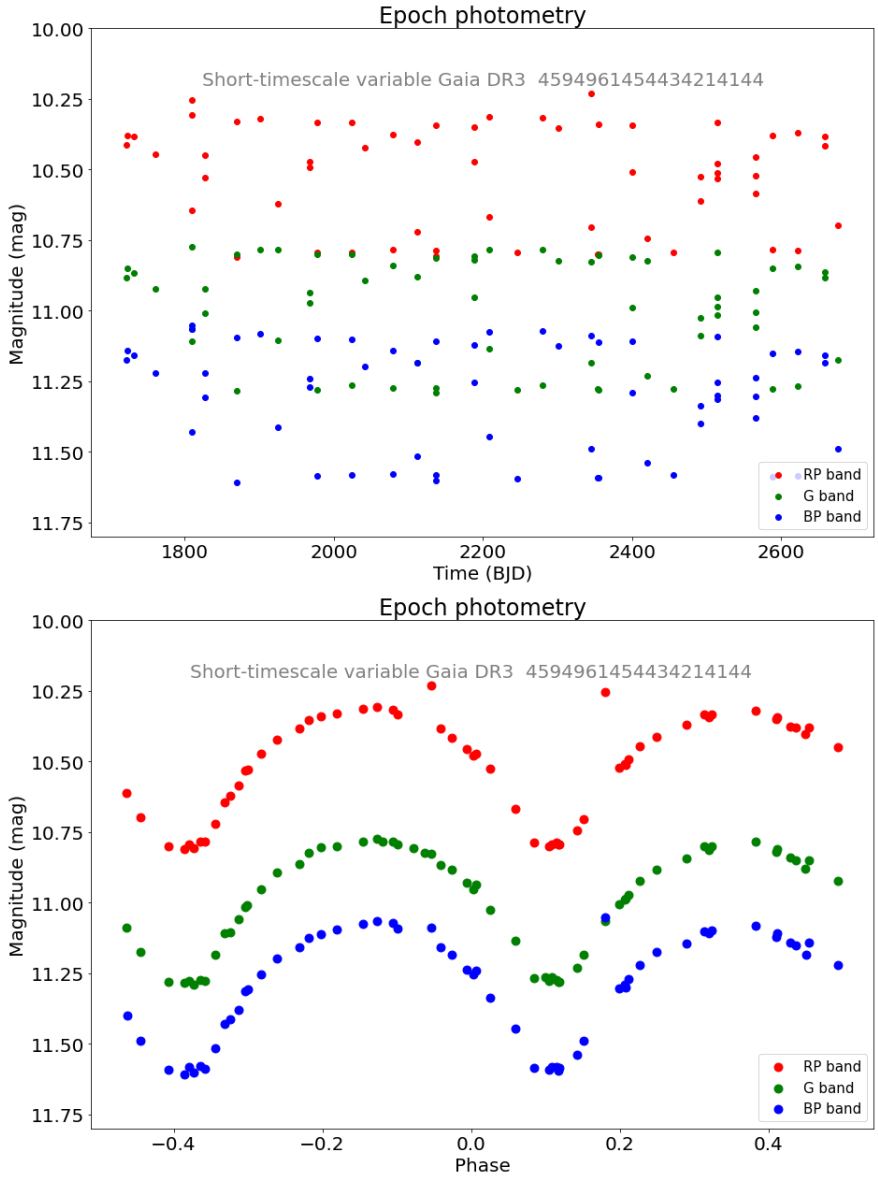

Figure 3.34: Light curve for the short-timescale binary star Gaia DR3 4594961454434214144 in the time domain (top) and in the phase domain (bottom).

3.8 Long period variables

Long period variables (LPV) are typically stars from the asymptotic giant branch (AGB) and the red giant branch (RGB) who show large variability amplitudes, in particular in the visual range, and periods ranging from a few tens of days to 1000 d (Lebzelter, T. et al. 2022).
The Gaia DR3 catalogue contains 1 720 558 LPV candidates, but only one of them is included in the all-sky PLATO Input Catalogue.
This source, identified as Gaia DR3 3005222633152619904 and EM* AS 119, is a cool, carbon-rich T Tauri giant star of spectral type B3IV[e].
Its time series in the Gaia photometric bands and its phase-folded light curve according to the tentative period P = 100 d are reported in figure 3.35.

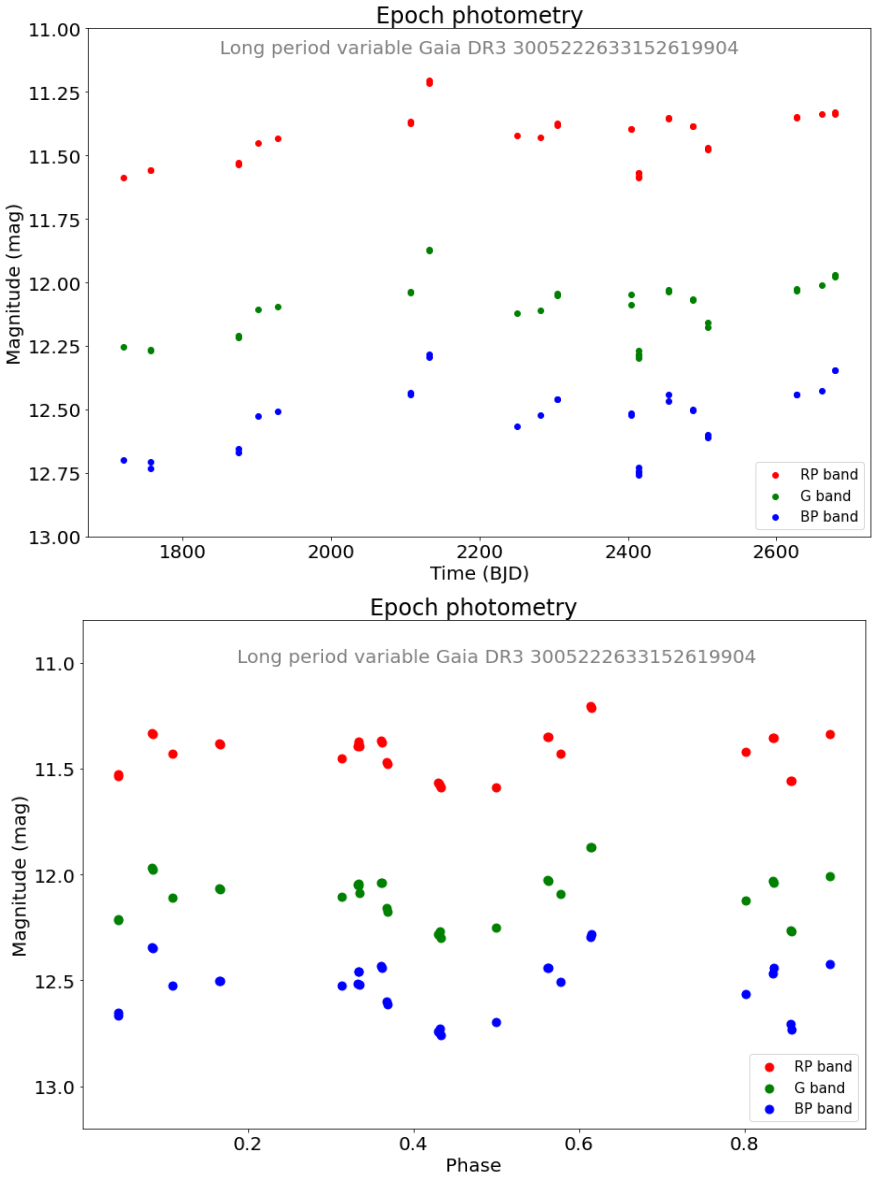

Figure 3.35: Time series (top) and phase-folded lightcurve (bottom) in the G, G_{BP} and G_{RP} bands for the long period variable Gaia DR3 3005222633152619904.

3.9 Cepheids

Cepheids are a class of periodic variable objects marked by a strong correlation between their absolute magnitude and period, which makes them standard candles to measure extra galactic distances, similarly to RR Lyrae stars. They can be classified as classical Cepheids (δ Cep), type II Cepheids (T2CEPs) and anomalous Cepheids (ACEPs).

The first family is the most populated and significant one: δ Cep are typically luminous, young (50-500 Myr) and massive (M $\approx$ 3–11 $M\odot$) stars, that can be used to test stellar evolution models, trace the metallicity gradient of the Milky Way, and model the galactic thin disc (Ripepi et al. 2022).

Among 15 000 Cepheids included in the Gaia DR3 variable objects collection, only one of them figures in the PLATO Input Catalogue: this source is the δ Cep Gaia DR3 4301612233202961024, whose first overtone pulsation period is P = 0.219 d. Its photometric time series and phase-folded lightcurve are displayed in figure 3.36.

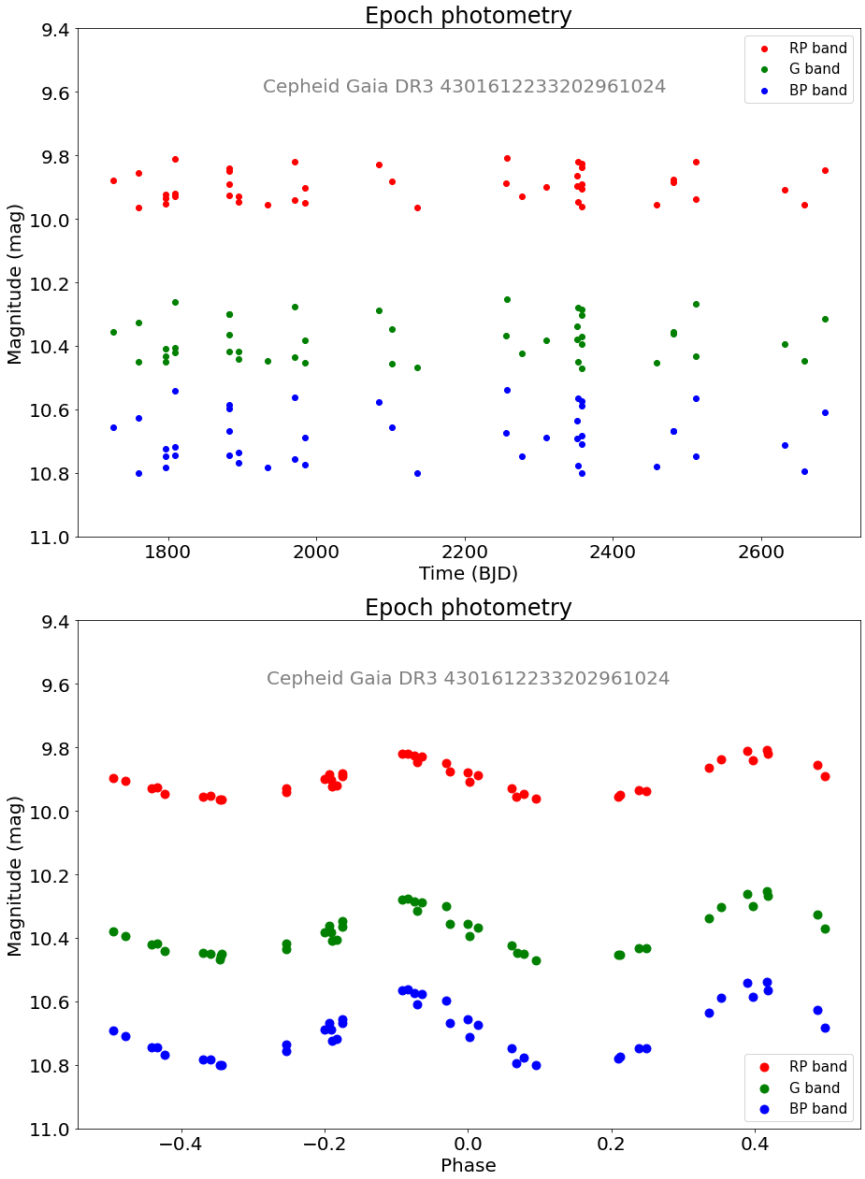

Figure 3.36: Time series (top) and phase-folded lightcurve (bottom) in the G, G_{BP} and G_{RP} bands for the Cepheid Gaia DR3 4301612233202961024 over the first overtone period P = 0.219 d.

Chapter 4

Cross-matching catalogues

4.1 Section Title

(Gavras et al. 2022)

Chapter 5

Conclusion

Appendix A

Appendix Title

Appendix

Bibliography

Montalto, M. et al. (2021). "The all-sky PLATO input catalogue". In: *Astronomy & Astrophysics* 653, A98. DOI: 10.1051/0004-6361/202140717.

Nascimbeni, V. et al. (2022). "The PLATO field selection process". In: *Astronomy & Astrophysics* 658, A31. DOI: 10.1051/0004-6361/202142256.

Gaia Collaboration, T. Prusti, et al. (2016). "The Gaia mission". In: *Astronomy & Astrophysics* 595, A1. DOI: 10.1051/0004-6361/201629272.

Gaia Collaboration, A. Vallenari, et al. (2022). *Gaia Data Release 3: Summary of the content and survey properties*. DOI: 10.48550/arXiv.2208.00211.

Rimoldini, Lorenzo et al. (2022). *Gaia Data Release 3: All-sky classification of 12.4 million variable sources into 25 classes*. DOI: 10.48550/arXiv.2211.17238.

Eyer, L. et al. (2022). *Gaia Data Release 3. Summary of the variability processing and analysis*. DOI: 10.48550/arXiv.2206.06416.

Clementini, G. et al. (2022). "Gaia Data Release 3. Specific processing and validation of all-sky RR Lyrae and Cepheid stars. The RR Lyrae sample". In: *A&A*. DOI: 10.1051/0004-6361/202243964.

Distefano, E. et al. (2022). "Gaia Data Release 3. Rotational modulation and patterns of color variations in solar-like variables". In: *A&A*. DOI: 10.1051/0004-6361/202244178.

Gaia Collaboration, De Ridder, J., et al. (2022). "Gaia Data Release 3. Pulsations in main-sequence OBAF-type stars". In: *A&A*. DOI: 10.1051/0004-6361/202243767.

Panahi, Aviad et al. (July 2022). "The detection of transiting exoplanets by Gaia". In: *Astronomy & Astrophysics* 663, A101. DOI: 10.1051/0004-6361/202243497.

Gaia Collaboration, F. Arenou, et al. (2022). *Gaia Data Release 3: Stellar multiplicity, a teaser for the hidden treasure*. arXiv: 2206.05595 [astro-ph.SR].

Mowlavi, N. et al. (2022). *Gaia Data Release 3. The first Gaia catalogue of eclipsing binary candidates*. arXiv: 2211.00929 [astro-ph.SR].

Roelens, M. et al. (Dec. 2018). "Gaia Data Release 2. Short-timescale variability processing and analysis". In: *Astronomy & Astrophysics* 620, A197. DOI: 10.1051/0004-6361/201833357.

Lebzelter, T. et al. (2022). "Gaia Data Release 3. The second Gaia catalogue of long-period variable candidates". In: *A&A*. DOI: 10.1051/0004-6361/202244241.

Ripepi, V. et al. (2022). *Gaia DR3: Specific processing and validation of all-sky RR Lyrae and Cepheid stars – The Cepheid sample*. arXiv: 2206.06212 [astro-ph.SR].

Gavras, P. et al. (2022). *Gaia Data Release 3: Cross-match of Gaia sources with variable objects from the literature*. DOI: 10.48550/arXiv.2207.01946.